

RESEARCH ARTICLE

Retinoic acid regulates pyruvate dehydrogenase kinase 4 (*Pdk4*) to modulate fuel utilization in the adult heart: Insights from wild-type and β -carotene 9',10' oxygenase knockout mice

Chelsee Holloway^{1,2,3} | Guo Zhong⁴ | Youn-Kyung Kim^{2,3} | Hong Ye^{2,3,5} |
Harini Sampath^{3,5} | Ulrich Hammerling^{2,3} | Nina Isoherranan⁴ |
Loredana Quadro^{2,3} 

¹Graduate Program in Endocrinology and Animal Bioscience, Rutgers University, New Brunswick, New Jersey, USA

²Department of Food Science, Rutgers University, New Brunswick, New Jersey, USA

³Rutgers Center for Lipid Research and Institute of Food Nutrition and Health, Rutgers University, New Brunswick, New Jersey, USA

⁴Department of Pharmaceutics Health Sciences, University of Washington, Seattle, Washington, USA

⁵Department of Nutritional Sciences, Rutgers University, New Brunswick, New Jersey, USA

Correspondence

Loredana Quadro, Department of Food Science, Rutgers University, 65 Dudley Road, New Brunswick, NJ 08901, USA.
Email: lquadro@sebs.rutgers.edu

Funding information

HHS | NIH | Eunice Kennedy Shriver National Institute of Child Health and Human Development (NICHD), Grant/Award Number: R01 HD094778; HHS | NIH | National Institute of Diabetes and Digestive and Kidney Diseases (NIDDK), Grant/Award Number: DK126963; HHS | NIH | National Institute of General Medical Sciences

Abstract

Regulation of the pyruvate dehydrogenase (PDH) complex by the pyruvate dehydrogenase kinase PDK4 enables the heart to respond to fluctuations in energy demands and substrate availability. Retinoic acid, the transcriptionally active form of vitamin A, is known to be involved in the regulation of cardiac function and growth during embryogenesis as well as under pathological conditions. Whether retinoic acid also maintains cardiac health under physiological conditions is unknown. However, vitamin A status and intake of its carotenoid precursor β -carotene have been linked to the prevention of heart diseases. Here, we provide in vitro and in vivo evidence that retinoic acid regulates cardiac *Pdk4* expression and thus PDH activity. Furthermore, we show that mice lacking β -carotene 9',10'-oxygenase

Abbreviations: *Alcat1*, acyl-CoA:lysocardiolipin acyltransferase-1; *Atp6*, mitochondrially encoded ATP synthase subunit 6; *BCO1*, β -carotene 15,15'-oxygenase; *BCO2*, β -carotene 9',10'-oxygenase; *Bco2^{-/-}*, β -carotene 9',10'-oxygenase deficient mice; *CPT*, carnitine palmitoyltransferase; *CytoxII*, cytochrome c oxidase subunit 2; *Dgat*, diglyceride acyltransferase; *Dhrs3*, dehydrogenase/reductase superfamily member 3; *Drp1*, dynamin-related protein; *Fas*, fatty acid synthase; *Fis1*, mitochondrial fission; *Glut*, glucose transporter; *Gpx*, glutathione peroxidase; *Hsl*, hormone-sensitive lipase; *Lpl*, lipoprotein lipase; *LRAT*, lecithin:retinol acyltransferase; *Mcd*, malonyl-CoA decarboxylase; *Mct*, monocarboxylate transporter; *Mfn1*, mitofusin 1; *NAC*, N-Acetylcysteine; *Nd5*, NADH dehydrogenase 5; *Nox*, NADPH oxidase complex; *OXPXOS*, oxidative phosphorylation; *Pdp*, pyruvate dehydrogenase phosphatase; *Pdk4*, pyruvate dehydrogenase kinase 4; *Pgc1 α* , peroxisome proliferator-activated receptor gamma coactivator 1-alpha; *Ppar*, peroxisome proliferator-activated receptor; *PrxIII*, peroxiredoxins; *P22phox*, cytochrome b558 α subunit; *RA*, retinoic acid; *RAR*, retinoic acid receptor; *RARE*, retinoic acid responsive element; *Rdh*, retinol dehydrogenase; *Raldh*, retinaldehyde dehydrogenase; *RE*, retinyl esters; *ROH*, retinol; *RXR*, retinoic acid X receptor; *Sod*, superoxide dismutase; *Scd1*, Stearoyl-CoA Desaturase 1; *Srebp1c*, sterol regulatory element-binding protein 1.

Guo Zhong and Youn-Kyung Kim contributed equally to this work.

This is an open access article under the terms of the [Creative Commons Attribution-NonCommercial-NoDerivs License](#), which permits use and distribution in any medium, provided the original work is properly cited, the use is non-commercial and no modifications or adaptations are made.

© 2022 The Authors. *The FASEB Journal* published by Wiley Periodicals LLC on behalf of Federation of American Societies for Experimental Biology.

(NIGMS), Grant/Award Number: GM111772; NIH F31 Ruth Kirschstein Predoctoral individual research award, Grant/Award Number: 1F31HL143930; Rutgers Center for Lipid Research small grant program; USDA, Hatch Project, Grant/Award Number: 1018402

(BCO2), the only enzyme of the adult heart that cleaves β -carotene to generate retinoids (vitamin A and its derivatives), displayed cardiac retinoic acid insufficiency and impaired metabolic flexibility linked to a compromised PDK4/PDH pathway. These findings provide novel insights into the functions of retinoic acid in regulating energy metabolism in adult tissues, especially the heart.

KEY WORDS

heart, metabolic flexibility, retinoic acid, β -carotene 9',10'-dioxygenase

1 | INTRODUCTION

To power a steady rhythm, the human heart draws three-quarters of its energy from lipids,¹ the balance being covered by a variety of sources, including glucose that feeds into the pyruvate dehydrogenase (PDH) complex.^{2,3} Superimposing beta-oxidation of fatty acids with oxidation of pyruvate generates the metabolic flexibility necessary to accommodate any rapidly arising energy demands in this organ. PDH catalyzes the oxidative decarboxylation of glucose-derived pyruvate to acetyl-CoA and NADH. Phosphorylation of PDH by four isoforms of pyruvate dehydrogenase kinase (PDK1-4) inhibits the enzyme. Conversely, PDH is re-activated by dephosphorylation via two pyruvate dehydrogenase phosphatases (PDP1 and 2).⁴ Regulation of PDH activity by *Pdk4* expression is a key factor for maintaining cardiac metabolic flexibility.^{2,3} Phosphorylation of the PDH E1 alpha regulatory subunit by PDK4 attenuates the pyruvate flux into the TCA cycle and this is compensated by increased fatty acid oxidation that generates acetyl-CoA as an alternative to pyruvate decarboxylation.⁵ Multiple signals regulating the cardiac PDK4/PDH pathway have been identified,⁶⁻⁹ but others have yet to be fully appreciated.

Micronutrients have long been known to sustain heart health.¹⁰⁻¹² Vitamin A sufficiency, in particular, correlated with a low risk of cardiovascular diseases (CVD) and CVD-linked mortality.¹³⁻¹⁶ Prominent among the biological functions attributable to vitamin A is the transcriptional regulation by retinoic acid which binds nuclear retinoic acid receptors controlling the expression of hundreds of genes.¹⁷ Retinoic acid is indispensable for normal heart morphogenesis during embryonic development.¹⁸ Additionally, under pathological conditions in adult mice, retinoic acid-mediated signaling has been implicated in cardiac remodeling, including suppression of cardiac hypertrophic features.¹⁹⁻²¹ Whether and how retinoic acid signaling also pertains to the normal physiology of the adult heart remains to be established. Interestingly, retinoic acid was shown to directly regulate the expression of

Pdk4 in kidney cells and adipocytes,^{22,23} but whether this extends to the heart is still unclear.

Epidemiological studies have also implicated high carotenoid intake in the risk reduction of CVD and improved heart function.²⁴⁻²⁶ Among the hundreds of carotenoids existing in nature, β -carotene is the most abundant dietary source of vitamin A as it yields retinoids (vitamin A and its derivatives) upon enzymatic cleavage. Specifically, symmetric cleavage by the cytoplasmic β -carotene 15,15'-oxygenase (BCO1) gives rise to two molecules of retinaldehyde which converts to retinoic acid upon oxidation, or to retinol by reduction.²⁷ Esterification of retinol yields retinyl esters, the storage form of the vitamin.²⁸ β -carotene can also be cleaved asymmetrically by the mitochondria-localized enzyme β -carotene 9',10'-oxygenase (BCO2) yielding β -ionone and β -apo10'-carotenal.²⁷ The latter can serve as a precursor of retinoids but can also function as a transcriptional regulator per se.²⁹ BCO2 is the sole β -carotene cleavage enzyme expressed in the adult heart.³⁰ Loss of *Bco2* in mice has been linked to mitochondrial dysfunction, impaired lipid metabolism, and inflammation as well as increased cellular oxidative stress in the liver, hypothalamus, muscle, and adipose tissue.³¹⁻³⁵ Furthermore, loss of *Bco2* has been reported to impair retinoid homeostasis in both developing and adult tissues.^{36,37} Despite such prominence, the role of cardiac BCO2 in maintaining the health of the adult heart remains unexplored, as do the contributions of the cardiac carotenoid and/or retinoid metabolic pathways to the overall health of this organ.

Here, we demonstrate that retinoic acid regulates cardiac *Pdk4* and its direct target PDH. Furthermore, we show that mice with whole-body ablation of *Bco2* display cardiac retinoic acid insufficiency which results in deregulation of the PDK4/PDH pathway in the heart. By exploiting the constitutively low cardiac levels of retinoic acid of the *Bco2*^{-/-} mice we were able to uncover novel roles of retinoid and carotenoid metabolic pathways that regulate fuel utilization in the adult heart.

2 | MATERIALS AND METHODS

2.1 | Animals, husbandry, and tissue collection

Twelve- to 14-week-old wild-type (WT) and *Bco2*^{-/-} female mice of mixed genetic background (C57BL/6J × 129/Sv) were used in this study unless otherwise indicated. WT and *Bco2*^{-/-} mice generated by intercrossing *Bco2*^{+/−} mice were maintained as inbred lines through parallel breeding. The genetic background of these lines, tested with a Mouse 384 SNP panel (Jackson Laboratories, Bar Harbor, ME), was about 65% C57BL/6J and 35% 129/Sv in both lines. Mice had access *ad libitum* to a standard vitamin A sufficient chow diet (18IU vitamin A/g of diet; Prolab Isopro RMH 3000 5p75) and water throughout life and for the duration of the experiments unless otherwise indicated. Mice were maintained on a 12-h light/dark cycle (7:00 a.m.–7:00 p.m.). All mice were euthanized by CO₂ inhalation according to approved protocols between 9:30 a.m. and 11:30 a.m. Serum, liver, gastrocnemius muscle, and whole hearts (or left ventricle, LV) were collected. For LV collection, hearts were washed in PBS and trimmed of excess tissue (connective, atrial) and the right ventricle was removed under a dissecting microscope (Olympus SZ61). After being weighed, all tissues were snap-frozen on dry ice and stored at −80°C until further analysis. All experiments were conducted in accordance with the National Institutes of Health Guide for the Care and Use of Laboratory Animals, as reviewed and approved by the Rutgers University Animal Care and Use Committee.

2.2 | HPLC and LC–MS/MS analysis

HPLC analyses were performed to measure the concentrations of retinol and retinyl ester in the heart, serum, and liver of wild-type and *Bco2*^{-/-} female mice, as previously described.³⁸ Retinoic acid was measured in the heart, serum, and liver by LC/MS–MS analysis, as previously described³⁹ using an AB Sciex 5500 QTRAP Mass Spectrophotometer with an Agilent 1290 UHPLC. For the heart, briefly, the tissue was homogenized in 0.9% saline solution. The internal standard (2 μM all-*trans*-retinoic acid-d₅ stock), as well as acetonitrile, 1% formic acid, and hexanes, were added to the tissue homogenates to aid in the extraction of different retinoic acid isomers. The organic layer was harvested, evaporated under nitrogen, and resuspended in 60% acetonitrile for analysis.

2.3 | mRNA isolation and real-time RT-PCR analysis

RNA extraction from heart, liver and muscle tissues, cDNA synthesis, and real-time RT-PCR were performed

as previously described.⁴⁰ Briefly, for heart extraction, total RNA was isolated using RNAB according to the manufacturer's instructions (NC9270490, ThermoFisher, Rockford, IL, USA). RNA purity was determined by Nanodrop 2000 Spectrophotometer (ThermoFisher, Rockford, IL, USA). After reverse transcription to complementary DNA (cDNA), target gene mRNA expression was quantified by real-time RT-PCR using the Applied Biosystems QuantStudio 3 instrument (Applied Biosystem, US). Sequences for primers used in this study have been previously published^{22,36,40,41} or are listed in Table S1. Samples were run in duplicate; data were quantified using the 2^(−ΔΔCt) method and results were expressed as a fold change from the control wild-type or vehicle groups of the same genotype. Values of target gene expression were normalized relative to the reference gene TATA-binding protein (*Tbp*).

2.4 | Preparation of tissue extracts

To prepare whole heart tissue extracts for Western blot analysis and enzymatic activity assay, frozen mouse tissues were pulverized with a mortar and pestle under liquid nitrogen. The resulting tissue samples (100 mg) were homogenized in a 500 μl volume of buffer containing 150 mM NaCl, 1% NP40, 0.5% sodium deoxycholate, 0.1% SDS, 50 mM Tris pH 8.0 with freshly added 1 mM EGTA, 1 mM NaF, 1 mM EDTA and supplemented with protease inhibitor (cat.# A32965, Pierce, Rockford, IL, USA; containing AEBSF, aprotinin, bestatin, E-64, leupeptin, and pepstatin A) and phosphatase inhibitor (cat.# 04906837001, Roche, St. Louis, MO, USA) cocktails. Protein concentration was determined by the method of Bradford⁴² using bovine serum as the standard.

2.5 | Western blot analysis

Western blots were performed for 30 μg protein/sample loaded per well. Proteins from tissue extracts were separated on a 10%–12% SDS polyacrylamide gel. Antibodies for PDK4 (cat.# ab214938, Abcam, Cambridge, MA, USA), total pyruvate dehydrogenase (PDH) (cat.# 456600, ThermoFisher, Rockford, IL, USA), and phosphorylated PDH (p-PDH) at serine 293 (cat.# NB-11093479, Novus Biologicals, Centennial, CO, USA) and 300 (cat.# AP1064, EMD Millipore Calbiochem, Temecula, CA, USA), as well as antibodies for the OXPHOS complex (cat.# 458099, ThermoFisher, Rockford, IL, USA) and CPT2 (cat.# ABS85, Millipore Sigma, St. Louis, MO, USA) were employed for western blot analysis. All antibodies were used at a dilution of 1:1000 and overnight incubation. Protein signals were normalized to vinculin (antibody anti vinculin, cat ab155120, Abcam, Abcam, Cambridge, MA, USA) and/or to protein

loading assessed by staining the membrane with Ponceau S (Millipore Sigma, St. Louis, MO, USA). Goat anti-rabbit (cat.# 31466 ThermoFisher, Rockford, IL, USA) or goat anti-mouse secondary antibodies (cat.# 1705047 Biorad, Hercules, CA, USA) were used at 1:5000 dilution. Signals were imaged using a Bio-Rad Chemidoc XRS Molecular Imager system. The quantification of the blots was performed per densitometry with Quantity One software (Bio-Rad, Hercules, CA, USA). The anti-PDK4 antibody mentioned above was validated by western blots using hearts from a *Pdk4* knockout mouse strain kindly provided by Drs. Robert Harris at Indiana University School of Medicine and Ben Woolbright at Kansas City Medical Center.

2.6 | PDH complex activity assay

All the groups of mice ($n = 4/\text{group}$; ~12 weeks of age) employed to measure the PDH complex activity were fasted for 13 h and re-fed for 4 h prior to euthanasia. When a specific treatment was administered (BMS493 or retinaldehyde), the last treatment dose was given prior to the beginning of the re-feeding period. PDH complex activity assay was determined by measuring the conversion of NAD to NADH (molar extinction coefficient of $6.22 \times 10^3 \text{ M}^{-1} \text{ cm}^{-1}$) by following the increase in absorbance at 340 nm.⁴³ Reactions were set up at room temperature in a total volume of 0.2 ml containing 50 mM potassium phosphate buffer pH 8.0, 0.2 mM thiamine pyrophosphate, 2.5 mM NAD, 0.13 mM CoA, 2.6 mM cysteine HCl, 2 mM potassium pyruvate, 1 mM MgCl₂, and 80 µg of protein extracts. To prevent the interfering effects of lactate dehydrogenase activity, lactate dehydrogenase inhibitor oxamate (cat.# E43209, Sigma, St. Louis, MO, USA) was added to a final concentration of 25 mM to each reaction.⁴⁴ Reactions were initiated with the addition of the reaction mix. Accumulation of NADH was monitored using a Bio-Rad Model 680XR microplate reader. Enzyme assays were performed in triplicate of each sample with an average standard deviation of $\pm 6\%$. All assays were linear with time and protein concentration. A unit of enzyme activity was defined as the amount of enzyme that catalyzes the formation of 1 nmol of NADH/min under the assay conditions described above. Specific activity was defined as units/milligrams of protein.

2.7 | Cell culture and treatments

Rat embryonic ventricular cardiomyocyte H9C2 cells were obtained from the American Type Culture Collection (CRL-1446, ATCC, Manassas, VA, USA). Cells from passage 20 were cultured at 37°C with 5% CO₂ in 4.5 g/L

D-Glucose Dulbecco's modified eagle's medium (DMEM) (ThermoFisher, Rockford, IL, USA) with 10% fetal bovine serum (FBS), 100 U/ml penicillin and 100 mg/ml streptomycin added. The medium was refreshed every two days until confluence was reached. Cells were seeded at 60%–80% confluence in 6-well plates. Cells were placed in serum-free media for 4 h before performing both the time-course and dose-response treatments with all-*trans* retinoic acid (R2625, Millipore Sigma, St. Louis, MO, USA). Retinoic acid in 0.1% DMSO was added at a final concentration of 1 µM or vehicle control (0.1% DMSO) for the time course treatment (cells harvested at different times from 30 min to 8 h). For dose-response experiments, cells were treated with different concentrations of retinoic acid (from 1 nM to 1 µM) or vehicle control (0.1% DMSO) for 2 h prior to being harvested. Each cell culture experiment was carried out in triplicate.

2.8 | BMS493 administration in vivo

Five-week-old WT female mice were treated with the pan retinoic acid receptor antagonist, BMS493 (15 µg/g of body weight; Millipore Sigma, St. Louis, MO, USA) or vehicle (1% DMSO in corn oil) by daily oral gavage for two weeks ($n = 5/\text{group}$). Throughout the experiment, mice were maintained on the regular chow diet *ad libitum*. Mice were euthanized in the morning of day 14, 4 h after the last gavage dose of BMS493, and serum and tissues were collected as described above.

2.9 | Retinaldehyde administration in vivo

Sixteen-week-old WT female mice were administered all-*trans* retinaldehyde (0.5 µg/g of body weight; R2500, Millipore Sigma, St. Louis, MO, USA) or vehicle (1% DMSO in corn oil) by daily intraperitoneal injection for two weeks ($n = 3\text{--}4/\text{group}$). Throughout the experiment, mice were maintained on the regular chow diet and had *ad libitum* access to food and water. Mice were euthanized in the morning of day 14, 4 h after the last dose of retinaldehyde, and serum and tissues were collected as described above.

2.10 | N-Acetylcysteine (NAC) supplementation in vivo

Eleven-week-old WT and *Bco2*^{-/-} female mice ($n = 4\text{--}5/\text{genotype}$) were treated with the antioxidant NAC (A1540922, ThermoFisher, Rockford, IL, USA) at a dose

of 0.5 mg/g bodyweight in the drinking water for two weeks. Water was replaced every three days. Throughout the experiment, mice were maintained on a regular chow diet. At the end of the treatment, mice were euthanized between 9 a.m. and 11 a.m. and tissues were collected as described above.

2.11 | Glucose, lactate, triglyceride, and non-esterified fatty acid measurements

Blood glucose levels were measured in fasted (overnight for 12 h) and continuously fed mice with the AimStrip blood glucose monitoring system (Germaine Laboratories, San Antonio, TX). Serum total lactic acid (D-L-lactate) was measured by an enzymatic assay (Megazyme Ltd., Bray, Ireland), according to the manufacturer's recommendations. Heart lipid extracts or serum were used in the HR-Series NEFA HR and L-Type TG H kits (WAKO Chemicals, Richmond VA) to measure NEFAs and TGs, respectively, according to the manufacturer's instructions.

2.12 | Measurements of lipid content in the left ventricle by TLC GC-MS

Heart (LV) lipid extracts were also prepared by Folch extraction⁴⁵ to be analyzed by TLC GC-MS as described previously.^{46,47} Briefly, tissue extracts were dissolved in chloroform, 2% Triton X100 solution and subsequently evaporated under nitrogen and dissolved in water. Lipids were then separated by thin-layer chromatography (TLC) on silica gel-60 plates (Millipore Sigma, St. Louis, MO, USA) in heptane-isopropyl ether-glacial acetic acid (60:40:3, v/v/v) with authentic standards. Bands corresponding to TG, FFA, DAG, and PL standards were scraped off the plate and transferred to screw cap glass tubes containing pentadecanoic and heptadecanoic acids as internal standards. FAs were transmethylated in the presence of 14% boron trifluoride in methanol. The resulting methyl esters were extracted with hexane and analyzed by gas-liquid chromatography-mass spectrometry (GC-MS).

2.13 | Endurance test

Twelve-week-old WT and *Bco2*^{-/-} female mice ($n = 4$ /group) were acclimated to a speed-controlled treadmill that uses electric shock as a stimulus (Columbus Instruments, Columbus, OH) one day prior to test day and data collection. During the acclimation period, mice

were kept on the treadmill for 5 min at a speed of 6 meters (m)/min with a 0° incline. During the endurance test mice were run on the treadmill at a constant 25° incline, the speed increased from 6 m/min to 3 m/min every 3 min until the mice reached exhaustion which was reached when an individual mouse remained on the grid for more than 10 secs, despite the shock stimulus.

2.14 | Statistical analysis

Data for cell culture and in vivo experiments/measurements are presented as mean \pm standard deviation (SD) unless otherwise stated. The student's *t*-test was used to detect statistically significant differences between two groups for paired analysis. For the NAC experiment (four experimental groups) and the dose-response experiment in Figure 1, data were normally distributed (as assessed by Shapiro Wilk Test) and analyzed with a two-way or one-way analysis of variance (ANOVA), respectively, followed by a Tukey's post hoc test. SPSS statistical software (IBM SPSS Statistics, version 23; SPSS, Inc.) was used for statistical analyses. $p \leq .05$ was regarded as statistically significant.

3 | RESULTS

3.1 | *Pdk4* mRNA expression is regulated by retinoic acid in the heart

Retinoic acid is known to transcriptionally upregulate the *Pdk4* gene directly in adipocytes and kidney cells, through two retinoic acid responsive elements (RARE) located within its promoter.^{22,23} To determine whether such transcriptional upregulation also takes place in the heart, we treated H9C2 rat cardiomyocytes with retinoic acid (1 μ M) for different time periods. *Pdk4* mRNA levels began to increase as early as 30 min post-treatment, rising to a 20-fold maximum within 2 h (Figure 1A). mRNA levels of *Cyp26b1*, one of the enzymes that oxidize retinoic acid into inactive metabolites,⁴⁸ increased in parallel in a time-dependent manner, reaching the highest expression after 8 h (Figure 1B). mRNA levels of both *Pdk4* (Figure 1C) and *Cyp26b1* (Figure 1D) also increased in a dose-dependent manner compared to vehicle. *Cyp26A1*, another retinoic acid catabolizing enzyme,⁴⁸ was expressed at low levels in the H9C2 cardiomyocytes but did not respond to retinoic acid treatment (data not shown).

To evaluate whether cardiac *Pdk4* expression is regulated by retinoic acid *in vivo*, we inhibited retinoic acid signaling by the retinoic acid receptor (RAR) pan-antagonist, BMS493.⁴⁹ Five-week-old WT females were orally gavaged with BMS493 (15 μ g/g body weight) or vehicle (1% DMSO in corn oil), daily for two weeks. BMS493

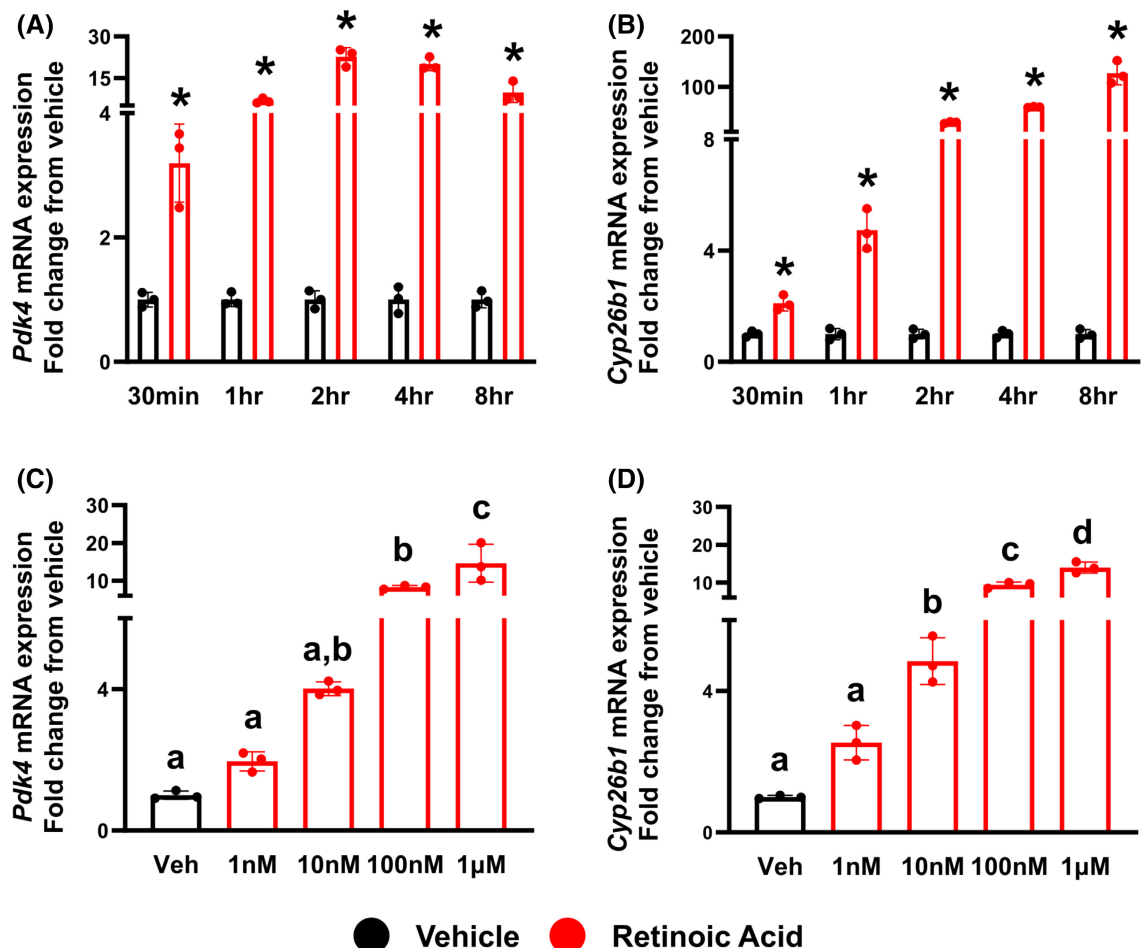


FIGURE 1 *Pdk4* is transcriptionally regulated by retinoic acid in H9C2 cardiomyocyte cells. Real-time RT-PCR analysis of *Pdk4* (A and C) and *Cyp26b1* (B and D) in H9C2 cells treated with 1 μM all-trans-retinoic acid (RA) from 30 min to 8 h (A and B) or treated for 2 h with increasing concentrations of RA (from 1 nM to 1 μM) (C and D). Each experiment was conducted in triplicate. Values are expressed as mean ± SD and calculated using the $2^{-\Delta\Delta CT}$ method. In panels (A) and (B), statistical analysis by *t*-test; * $p \leq .05$ versus the corresponding vehicle-treated group at each specific time point. In panels (C) and (D), statistical analysis by one-way ANOVA; different letters indicate a significant difference ($p \leq .05$) among the different groups.

treatment attenuated cardiac *Pdk4* mRNA (Figure 2A) and protein (Figure 2B) expression levels without adverse effects on mice (data not shown). To corroborate the efficacy of BMS493 in the heart we monitored the cardiac expression of *Cyp26a1* and *Cyp26b1*, as well as the retinoic acid receptor *Rarβ*. Expression of all three genes was attenuated (Figure 2A), as expected.^{48,50,51} Interestingly, *Pdk4* mRNA expression in liver and gastrocnemius muscle remained unaffected by the BMS493 treatment, despite a significant reduction of *Cyp26a1* and *Cyp26b1* expression in these organs (Figure S1A,B). To learn whether the reduction of PDK4 levels had functional consequences, we tested the phosphorylation status of the PDH E1 alpha regulatory subunit, the primary target of PDK4.⁴⁴ Indeed, the two primary inhibitory serine sites of the PDH E1 alpha subunit known as direct targets of PDK4 (S293 and S300)⁴⁴ were partially de-phosphorylated in the heart of the BMS493-treated mice compared to those of WT mice

(Figure 2C). The activity of the PDH complex was also directly assessed as detailed in the Materials and Methods. To maximize the contribution of PDK4 to PDH phosphorylation,⁵² mice were fasted for 13 h and re-fed for 4 h prior to sacrifice. In agreement with the phosphorylation levels, the enzymatic activity of the PDH complex in the heart of the WT females treated with BMS493 was significantly increased compared to the vehicle-treated group (Figure 2D).

Next, 16-week-old WT mice were treated with retinaldehyde (0.5 μg/g body weight) or vehicle (1% DMSO in corn oil) for two weeks by intraperitoneal injection. Treatment with the precursor of retinoic acid,^{53,54} upregulated cardiac *Pdk4* mRNA (Figure 2E) and protein levels (Figure 2F), and at the same time increased cardiac expression of *Cyp26a1* and *Cyp26b1* (Figure 2E). We showed that the phosphorylation levels of the PDH E1 alpha subunit at S293 and S300 were partially increased (Figure 2G)

whereas the enzymatic activity (measured as above) was attenuated (**Figure 2H**) in the heart of the retinaldehyde-treated WT female mice compared to those of the vehicle-treated group. Finally, as in the heart, expressions of *Cyp26a1* and *Cyp26b1* were significantly enhanced in the liver (**Figure S2A**) and gastrocnemius muscle (**Figure S2B**). Interestingly, whereas hepatic *Pdk4* expression increased, muscle *Pdk4* mRNA expression was not affected by the retinaldehyde treatment (**Figure S2A,B**).

Together, these findings strongly indicated that retinoic acid upregulates *Pdk4* in the heart of female mice.

3.2 | The heart of the *Bco2^{-/-}* mice displays retinoid insufficiency

The literature indicates that the lack of *Bco2* impacts retinoid homeostasis in the adult liver³⁷ and developing tissues³⁶ in the absence of dietary carotenoid supplementation. In these studies, tissue retinoic acid levels were not directly measured, and the underlying mechanisms remain unexplained. We analyzed retinoid levels in serum, liver, and heart of mutant and WT female mice by HPLC³⁸ and LC-MS/MS.³⁹ HPLC analyses revealed no differences in retinol and retinyl ester levels in the mutant hearts (**Table 1**). By contrast, serum and liver retinol levels were slightly but significantly reduced in the *Bco2^{-/-}* mice, whereas hepatic retinyl ester concentrations were not different between the two strains (**Table 1**). Notably, LC-MS/MS analysis revealed reduced levels of retinoic acid in the hearts of the mutants compared to the WT control group (**Figure 3A**). This reduction was cardiac-specific as there was no difference in hepatic retinoic acid levels between genotypes (**Figure 3B**). Serum retinoic acid levels trended to be higher in the mutant mice compared to WT mice ($p = .08$; **Figure 3C**). These data clearly indicated cardiac retinoic acid insufficiency in the heart of the mutant mice.

To further probe for disturbed retinoid homeostasis in this organ, we measured cardiac mRNA levels of key genes of retinoid biosynthesis whose vitamin A-dependent expression is considered to reflect the flux of retinoids within tissues.⁵⁵ Retinol dehydrogenase 1 (*Rdh1*), which converts retinol to retinaldehyde, and retinaldehyde dehydrogenase 1 (*Raldh1*), which converts retinaldehyde to retinoic acid,^{53,54} were significantly upregulated in the mutant hearts (**Figure 3D**). In contrast, the genes that catabolize retinoic acid⁴⁸ either showed a significant downregulation (*Cyp26a1*) or remained unchanged (*Cyp26b1*) (**Figure 3D**). Surprisingly, lecithin:retinol acyltransferase (*Lrat*), which converts retinol to retinyl esters²⁸ was significantly upregulated in the hearts of *Bco2^{-/-}* mice (**Figure 3D**). Except for the latter, these data suggested a potential enhancement of the retinoic acid biosynthesis pathway that we interpreted

as a compensatory mechanism for counteracting the cardiac retinoic acid insufficiency of the *Bco2^{-/-}* mice.

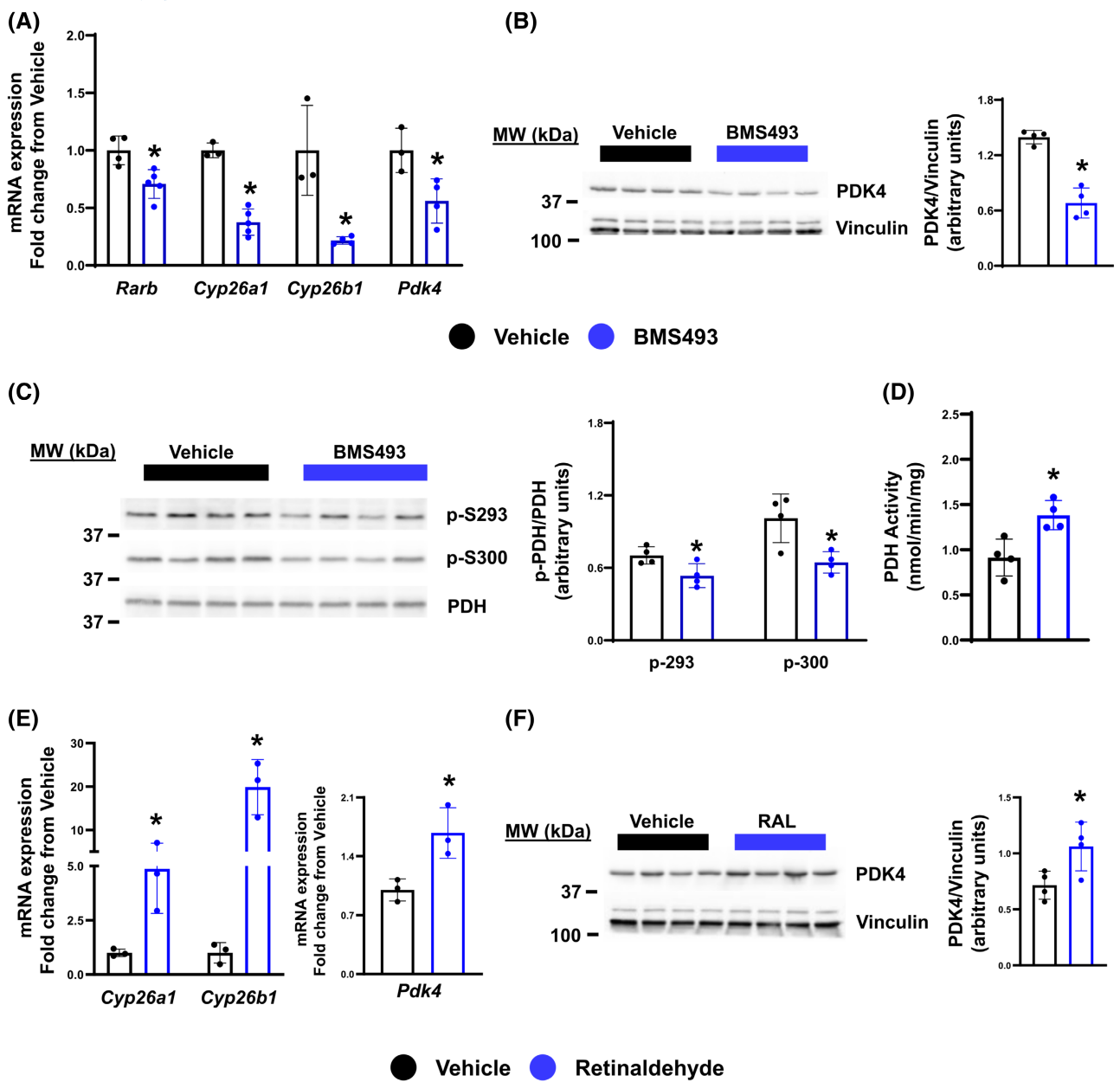
3.3 | Loss of *Bco2* impairs cardiac PDK4-mediated regulation of PDH activity

We next asked whether the reduced retinoic acid levels in the heart of the mutant females affected the PDK4-dependent regulation of the PDH complex activity. Cardiac *Pdk4* mRNA (**Figure 4A**) and protein (**Figure 4B**) were significantly downregulated in the *Bco2^{-/-}* females compared to WT age-matched controls. None of the other three PDK isoforms that normally modulate PDH activity was differentially expressed in the heart of the mutants compared to WT (**Figure S3**). The expression of the phosphatase *Pdp1* (**Figure 4C**), but not *Pdp2* (**Figure S3**), was slightly but significantly upregulated in the hearts of the *Bco2^{-/-}* mice. Importantly, *Pdk4* mRNA was also downregulated at pre-puberty in the heart of four-week-old *Bco2^{-/-}* females compared to WT age-matched controls (**Figure S4A**). Finally, consistent with the reduced cardiac *Pdk4* expression, the phosphorylation of PDH E1 alpha subunit at S293 and S300 was also reduced (**Figure 4D**), and the enzymatic activity of the PDH complex (assayed as indicated above) was significantly increased in the heart of the female mutants compared to age- and sex-matched WT controls (**Figure 4E**).

Interestingly, in mice lacking *Bco2*, *Pdk4* mRNA expression was downregulated in the liver (**Figure S4B**) but not in the skeletal muscle tissue (gastrocnemius) (**Figure S4C**). Given that hepatic *Pdk4* expression was not affected by BMS493 in WT mice (**Figure S1A**), we reasoned that the regulation of *Pdk4* may be transcriptionally dependent on retinoic acid only in the heart. Overall, these data suggested an organ-specific impact of BCO2 on the PDK4/PDH pathway.

3.4 | Cardiac retinoic acid insufficiency in the *Bco2^{-/-}* mice is linked to mitochondria dysfunctions

We next wondered why the mutant heart was retinoic acid insufficient. The literature indicates that loss of the mitochondria localized BCO2 enzyme in mice leads to increased cellular oxidative stress and mitochondrial dysfunctions, at least in the liver, hypothalamus, adipose, and muscle.^{31-35,56} To gain insights into potential cardiac mitochondrial deficits in the mutants, we first measured mitochondrial DNA content in the heart. No differences were found between WT and *Bco2^{-/-}* females in the expression of *Atp6*, *CytoxII*, and *Nd5* (**Figure 5A**) by real time RT-PCR



analysis. Notably, the levels of the protein complexes of the oxidative phosphorylation chain in the heart were also similar between genotypes, as assessed by western blot analysis (Figure 5B). In view of expected oxidative stress

in the tissues of the mutant mice, we measured the expression of mitochondrial encoded genes associated with repair, i.e., fission, fusion and mitophagy.⁵⁷ Interestingly, the expression of the fusion gene *Mfn1* was slightly but

FIGURE 2 *Pdk4* is transcriptionally regulated by retinoic acid signaling in the WT heart *in vivo*. (A–D) BMS493-treated or -untreated 5-week-old WT female mice. (A) mRNA expression of *Rarb*, *Cyp26a1*, *Cyp26b1*, and *Pdk4* is measured by real-time RT-PCR in the whole heart ($n = 3\text{--}4$ mice/group). Values are calculated using the $2^{-\Delta\Delta CT}$ method and expressed as mean \pm SD. Immunoblot and quantification of (B) PDK4 (47 kDa) and (C) phospho-PDH E1 (47 kDa) at Serine 300 and 293 in the whole heart ($n = 4$ mice/group). (D) PDH enzymatic activity is measured as detailed in the Materials & Methods section. Each value represents the activity of individual animals. The assay was performed in triplicate. (E–H) Retinaldehyde (RAL)-treated or -untreated 16-week-old WT female mice. (E) mRNA expression of *Cyp26a1*, *Cyp26b*, and *Pdk4* is measured by real-time RT-PCR in the whole heart ($n = 3\text{--}4$ mice/group). Values are calculated using the $2^{-\Delta\Delta CT}$ method and expressed as mean \pm SD. (F) Immunoblot and quantitation of PDK4 (47 kDa; $n = 4$ mice/group) and (G) phospho-PDH E1 (47 kDa) at Serine 300 and 293 in the whole heart ($n = 4$ mice/group). (H) PDH enzymatic activity is measured as detailed in the Materials & Methods section. Each value represents the activity of individual animals. The assay was performed in triplicate. Levels of vinculin (118 kDa) were used as the loading control in B and F. Values are expressed as mean \pm SD. Statistical analyses by *t*-test between treated and untreated groups within each gene or protein; * $p \leq .05$.

TABLE 1 Retinol and retinyl ester concentrations in WT and *Bco2*^{−/−} female mice

	Serum ($\mu\text{g/dl}$)		Liver ($\mu\text{g/g}$)		Heart ($\mu\text{g/g}$)	
	Retinol	Retinyl ester	Retinol	Retinyl ester	Retinol	Retinyl ester
Wild-type	17.2 \pm 6.4	3.1 \pm 2.2	4.1 \pm 1.6	397.8 \pm 93.5	99.6 \pm 30.4	46.8 \pm 23.2
<i>Bco2</i> ^{−/−}	14.4 \pm 8.6*	5.9 \pm 4.8	2.7 \pm 1.4*	394.5 \pm 82.5	90.5 \pm 20.5	25.4 \pm 18.3

Note: HPLC analysis of serum, liver, and heart in 12–14-week-old WT and *Bco2*^{−/−} female mice. Values are as means \pm SD. $n \geq 8$ /group. Statistical analysis by *t*-test between genotypes within the same metabolite and tissue.

* $p \leq .05$.

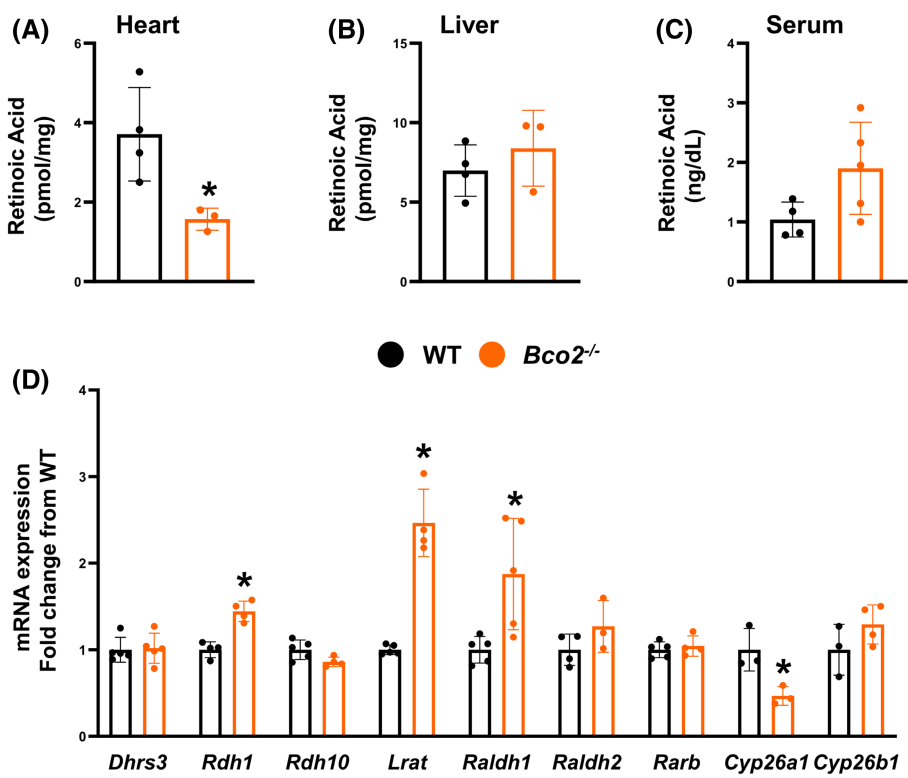


FIGURE 3 Retinoic acid concentrations and mRNA expression levels of critical regulators of the retinoid metabolic pathway in the *Bco2*^{−/−} mice. Retinoic acid (RA) concentrations were measured by LC-MS/MS in (A) whole heart, (B) liver, and (C) serum of 12–14-week-old WT and *Bco2*^{−/−} female mice ($n = 3\text{--}5$ mice/genotype). (D) Gene expression of *Dhrs3*, *Rdh1*, *Rdh10*, *Lrat*, *Raldh1*, *Raldh2*, *Rarb*, *Cyp26a1*, *Cyp26b1* measured by real-time RT-PCR in the heart (left ventricles) of WT and *Bco2*^{−/−} female mice ($n = 4\text{--}6$ mice/genotype). Values are expressed as mean \pm SD and calculated using the $2^{-\Delta\Delta CT}$ method. Statistical analysis by *t*-test between genotypes within each tissue (A–C) or gene (D); * $p \leq .05$.

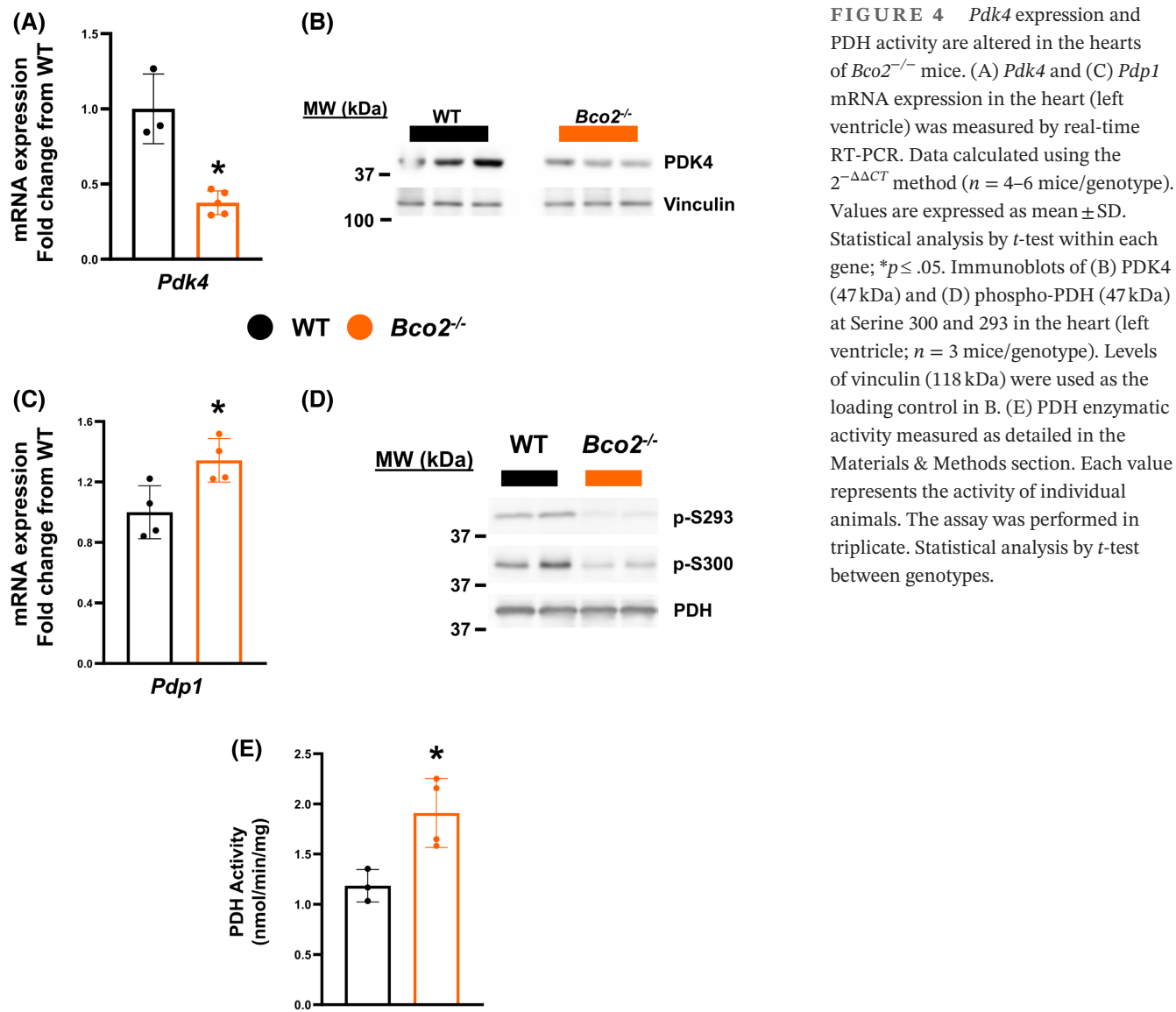


FIGURE 4 *Pdk4* expression and PDH activity are altered in the hearts of *Bco2*^{-/-} mice. (A) *Pdk4* and (C) *Pdp1* mRNA expression in the heart (left ventricle) was measured by real-time RT-PCR. Data calculated using the $2^{-\Delta\Delta CT}$ method ($n = 4-6$ mice/genotype). Values are expressed as mean \pm SD. Statistical analysis by *t*-test within each gene; * $p \leq .05$. Immunoblots of (B) PDK4 (47 kDa) and (D) phospho-PDH (47 kDa) at Serine 300 and 293 in the heart (left ventricle; $n = 3$ mice/genotype). Levels of vinculin (118 kDa) were used as the loading control in B. (E) PDH enzymatic activity measured as detailed in the Materials & Methods section. Each value represents the activity of individual animals. The assay was performed in triplicate. Statistical analysis by *t*-test between genotypes.

significantly decreased in the heart of the *Bco2*^{-/-} mice (Figure 5C). *Mfn1* deficiency is often used as an indicator of excessive ROS production in the heart⁵⁸ and elsewhere.^{59,60} Indeed, other oxidative stress markers, such as *Alcat1*, a regulator of cardiolipin function,⁶¹ and *p22phox*, a critical component of the NADPH oxidase or NOX complex,⁶² were slightly but significantly upregulated in the *Bco2*^{-/-} hearts (Figure 5D). Upregulation of *p22phox* is a major indicator of activation of the NOX complex which is a main source or generator of ROS,⁶² again implying increased ROS in the heart of the mutant strain. Therefore, we wondered whether such a pro-oxidant environment in the heart of the mutants favored the spontaneous oxidation of retinoic acid, reducing its tissue levels. We administered N-Acetylcysteine (NAC), a potent antioxidant and direct ROS scavenger⁶³ to WT and *Bco2*^{-/-} female mice, in the drinking water for two weeks. As predicted, the NAC treatment restored cardiac retinoic acid concentrations in

the mutants to the levels of the WT (Figure 5E). Moreover, *Pdk4* mRNA (Figure 5F) and protein (Figure 5G) expression levels increased in parallel in the heart of the NAC-treated *Bco2*^{-/-} mice compared to the untreated mutants. Overall, these findings strongly implied that the lack of cardiac Bco2 generated a pro-oxidative environment that resulted in retinoic acid insufficiency in this organ.

3.5 | Dysregulation of lipid and glucose metabolism in the heart of the *Bco2*^{-/-} mice

The decreased *Pdk4* expression and the consequent increased activity of the PDH complex in the heart of the mutant females implied a shift in the energy-providing substrate from lipids to glucose. To gain insights into this potential metabolic dysregulation we measured fasting

(Figure 6A) and fed (Figure 6B) serum glucose levels. We found these to be significantly reduced in *Bco2*^{-/-} female mice only in the fed state (Figure 6B). Furthermore, mutant mice showed slightly higher serum levels of lactate, the main byproduct of glycolysis (Figure 6C), suggesting increased glycolysis and efflux of lactate across the plasma membrane.⁶⁴ We took these data as an indication of potentially increased glucose uptake and glycolysis.⁶⁴ In agreement with this interpretation, cardiac gene expression of the constitutive glucose transporter *Glut1*, but not *Glut4*, was higher in the *Bco2*^{-/-} mice (Figure 6D), as was the expression of the monocarboxylate transporter *Mct1* (Figure 6D).

We next measured lipid concentrations in serum and heart of WT and mutant mice. Serum triglycerides (TG) but not non-esterified fatty acids (NEFA) were significantly lower in the mutants (Figure 7A,B). GC-MS analysis of various lipid species in the heart of *Bco2*^{-/-} versus WT mice revealed a modest but significant reduction in TG content, without significant differences in other classes of lipids, such as diacylglycerols, phospholipids, or cholesteryl esters between genotypes (Figure 7C). Note that the reduction in cardiac TG levels was independently confirmed in a separate group of mice by using a commercial kit (1975.8 ± 399.0 and 1130.8 ± 297.1 mg/dl in WT and *Bco2*^{-/-} mice, respectively; $n = 5$ /genotype; $p = .04$ by *t*-test). Further analysis of the TG acyl chain distribution in the heart showed a significant reduction in 16:0 and 18:0 fatty acid species, as well as in those with 18 carbons and various degrees of unsaturation (Table 2). We also measured mRNA and protein levels of key genes involved in lipid metabolism. Of the tested fatty acid uptake-related genes, only mRNA levels of *Cd36* (Figure 7D), but not its protein (data not shown), were slightly reduced in the heart of the mice lacking *Bco2*. Cardiac triglyceride synthesis seemed to be unaffected by the lack of *Bco2*, as inferred by unaltered mRNA expression of the acyl CoA:diacylglycerol acyltransferases, *Dgat1* and *Dgat2* (Figure 7D). In contrast, mRNA expression of *Srebp1c*, a key lipogenic transcription factor,⁶⁵ and of *Scd4*, the cardiac-specific stearoyl-CoA desaturase that catalyzes the conversion of saturated fatty acids (especially 18:0 and 16:0) into monounsaturated fatty acids,⁶⁶ were significantly reduced in the *Bco2*^{-/-} hearts (Figure 7D). The attenuation of *Scd4* is consistent with the observed reductions in n7- and n9-monounsaturated fatty acids within cardiac TGs (Table 2). These data suggested a potential downregulation of the lipid biosynthetic pathway in the mutant hearts, possibly to spare acetyl-CoA as a substrate for the TCA cycle. Although transcription of *Pgc1a*, the master regulator of mitochondrial energy production from lipids,⁶⁷ as well as the mRNA levels of the transcription factors *Ppara* and *Ppary* were not different between mutant and WT control hearts (Figure 7D), mRNA

expression of *Acadm*, a key enzyme in the beta-oxidation of medium-chain fatty acids,⁶⁸ was significantly decreased in the heart of *Bco2*^{-/-} mice. Moreover, the expression of *Cpt2*, one of the fatty acid transporters across the mitochondrial membrane and critical to mitochondria fatty acid oxidation⁶⁸ (Figure 7D), as well as its protein levels (Figure 7E), were slightly but significantly reduced in the heart of the *Bco2*^{-/-} females compared to WT controls. These data suggested a potential impairment of fatty acid oxidation in the heart of these mutants.

Overall, consistent with the reduced phosphorylation of the PDH E1 alpha subunit (Figure 4D) and hence its enhanced activity (Figure 4E) in the mutant hearts, these findings indirectly support the hypothesis that the *Bco2*^{-/-} adult heart relies mostly on carbohydrates as an energy source, concomitantly with reduced lipid availability and impaired beta-oxidation.

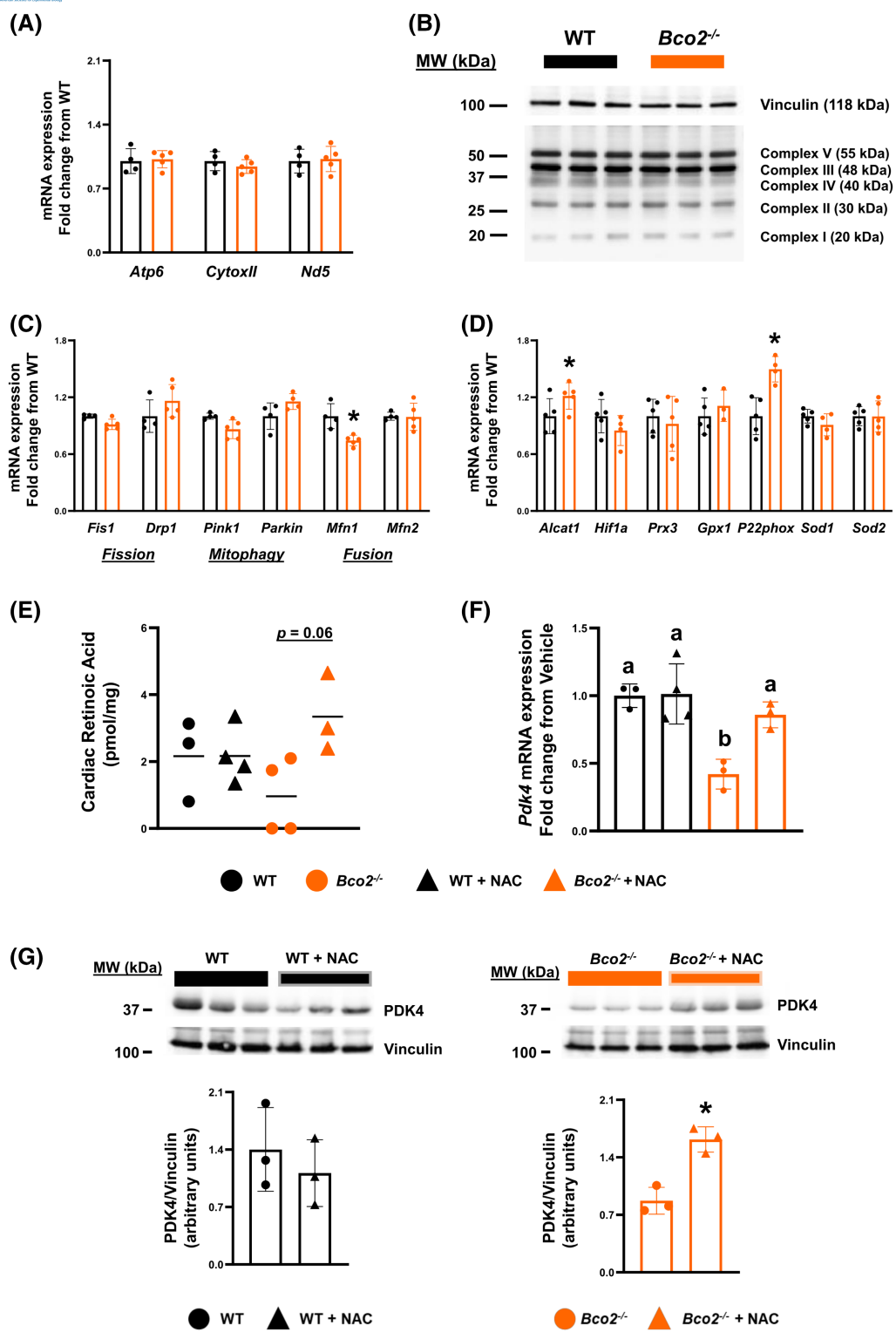
3.6 | Exercise endurance is markedly reduced in the *Bco2*^{-/-} mice

Given that the *Bco2*^{-/-} mice are viable, healthy, and fertile when reared under normal housing conditions and receive a regular chow diet,³⁶ we wondered whether the reduced activity of the PDH complex and the suggested metabolic deficit of the mutant heart would have consequences under conditions that require prompt adaptation to changing energy-providing substrates (lipid versus glucose). Indeed, the mutant mice showed a marked drop in exercise endurance, as their total running distance was reduced by approximately 40% compared to WT controls (Figure 7F).

4 | DISCUSSION

The goal of this study was to gain new insights into the role of retinoid and carotenoid metabolisms as potential contributors to adult heart health. This question stemmed from the literature indicating that (i) vitamin A status^{13,14,16} and intake of carotenoids^{24–26} positively correlate with low risk of cardiovascular diseases (CVD) and CVD-related deaths; (ii) perturbations of retinoic acid homeostasis and signaling often accompany heart pathological conditions^{19–21,69}; (iii) *Pdk4*, a key regulator of PDH activity and hence fuel allocation, is modulated by retinoic acid in liver, adipocytes, and kidney^{22,23}; (iv) mice lacking BCO2, the sole carotenoid cleavage enzyme expressed in the adult heart,³⁰ display altered tissue retinoid homeostasis and metabolic phenotypes.^{33,34,37,56,70}

Postnatal development is marked by a metabolic reprogramming that renders the adult heart more reliant on fatty acids as an energy source than on glucose, which



is instead the predominant fuel source for the developing heart.¹ The healthy adult heart acquires about 70% of its ATP from beta-oxidation.¹ For the balance, it can utilize multiple sources of energy-providing substrates to maintain proper function and remain responsive to changing energy demands. This process is known as cardiac metabolic flexibility.⁷¹ Cardiac metabolic flexibility is challenged when the heart loses the ability to use fatty acids

over glucose, despite unchanged substrate availability or energetic demands.⁷¹ Indeed, the failing heart exhibits increased reliance on glycolysis for ATP production.⁷² A recent report has also linked decreased cardiac retinoic acid levels with heart failure in humans.⁶⁹ Importantly, PDK4 has been identified as a key regulator of cardiac substrate utilization during pregnancy³ and adult life^{73,74} by its ability to modulate the activity of the pyruvate dehydrogenase

FIGURE 5 Mitochondrial functions and oxidative status are linked to retinoic acid insufficiency in the heart of the *Bco2^{-/-}* mice. (A) Assessment of mitochondrial DNA content via gene expression of *Atp6*, *CytoxII*, and *Nd5* measured by real-time RT-PCR in the heart (left ventricle) of WT and *Bco2^{-/-}* female mice ($n = 4$ –6 mice/genotype). Values are calculated using the $2^{-\Delta\Delta CT}$ method. (B) Immunoblot and quantification of the oxidative phosphorylation complexes I–V in the heart (left ventricle) of 12–14-week-old WT and *Bco2^{-/-}* female mice ($n = 3$ mice/genotype). (C) mRNA expression of genes regulating mitochondria dynamics (*Fis1*, *Drp1*, *Pink1*, *Parkin*, *Mfn1*, *Mfn2*) and (D) oxidative stress-related pathways (*Alcat1*, *Prx3*, *Gpx1*, *p22phox*, *Sod1*, *Sod2*) measured by real-time RT-PCR in the heart (left ventricle) of WT and *Bco2^{-/-}* female mice ($n = 4$ –6 mice/genotype). Values are calculated using the $2^{-\Delta\Delta CT}$ method. Values are mean \pm SD. Statistical analysis by *t*-test between genotypes within each gene; * $p \leq .05$. (E) Cardiac (whole heart) retinoic acid concentrations are measured by LC–MS/MS ($n = 3$ –4 mice/genotype) in vehicle- (drinking water), or NAC-supplemented WT and *Bco2^{-/-}* female mice. (F) *Pdk4* mRNA expression in the whole heart ($n = 4$ –6 mice/genotype) of vehicle or NAC-supplemented WT and *Bco2^{-/-}* female mice. Values are expressed as mean \pm SD. (G) Immunoblot and quantification of PDK4 (47 kDa) in the heart (left ventricle) of 12–14-week-old WT and *Bco2^{-/-}* female mice ($n = 3$ mice/genotype). Levels of vinculin (118 kDa) were used as the loading control. In E and F, normally distributed data were statistically analyzed with a two-way ANOVA. Different letters indicate a significant difference among the groups, $p \leq .05$.

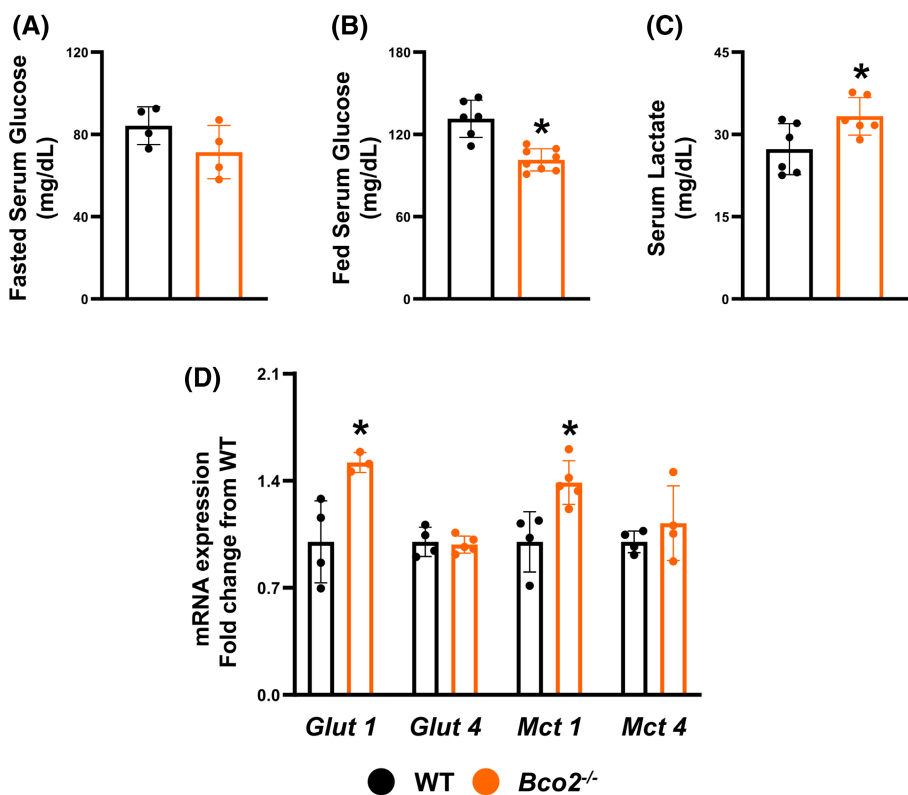


FIGURE 6 Markers of glucose metabolism in *Bco2^{-/-}* mice. (A, B) Serum glucose levels in fasted (12 h fasted) ($n = 4$ mice/genotype) and continuously fed ($n = 6$ –8 mice/genotype) 12–14 week-old WT and *Bco2^{-/-}* female mice. (C) Serum lactate ($n = 5$ mice/genotype) in 12–14 week-old WT and *Bco2^{-/-}* female mice. (D) mRNA expression levels of *Glut1*, *Glut4*, *Mct1*, and *Mct4* mRNA expression in the left ventricle of 12–14-week-old WT and *Bco2^{-/-}* female mice. Values are calculated using the $2^{-\Delta\Delta CT}$ method. Values are mean \pm SD. Statistical analysis by *t*-test between genotypes within each gene or metabolite; * $p \leq .05$.

(PDH) complex.⁵ We provided evidence that cardiac *Pdk4* expression is regulated by retinoic acid in vitro. Previous studies identified two functional RAREs in the promoter of *Pdk4* in the human embryonic kidney (HEK293)²² and mouse adipocytes (3T3-F442A) cells.²³ Here, we showed that *Pdk4* is induced in a time- and dose-dependent manner by retinoic acid in embryonic rat H9C2 cardiomyocytes, which are known to express both RAR and RXR receptors⁷⁵ (Figure 1). Our findings also demonstrated the

regulation of *Pdk4* expression by retinoic acid in the WT heart *in vivo*. Indeed, attenuation of retinoic acid signaling by the RAR pan-antagonist BMS493⁴⁹ caused diminished PDK4 mRNA and protein expression (Figure 2A,B) and significantly dephosphorylated the PDH E1 alpha subunit at the S293 and S300 regulatory sites (Figure 2C) increasing PDH activity (Figure 2D). Conversely, administration of the retinoic acid precursor retinaldehyde to WT mice increased cardiac PDK4 gene and protein expression

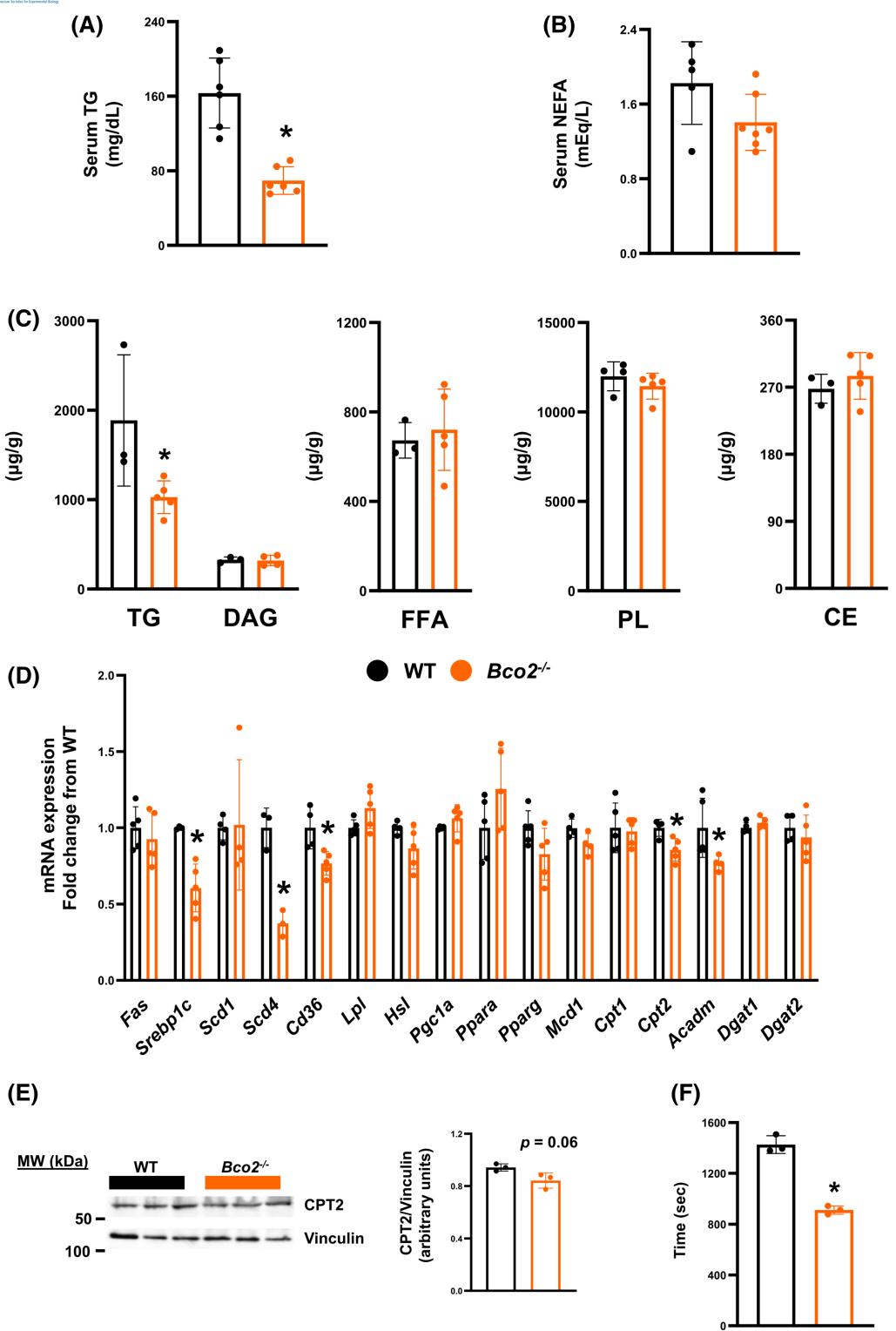


FIGURE 7 Lipid metabolic parameters and endurance capacity in *Bco2*^{-/-} mice. (A) Serum triglyceride (TG) ($n = 6\text{--}7$ mice/genotype) and (B) non-esterified fatty acid (NEFA) levels ($n = 5\text{--}8$ mice/genotype) in 12-14-week-old WT and *Bco2*^{-/-} female mice. (C) Cardiac lipid content by GC-MS analysis in 14-week-old WT and *Bco2*^{-/-} female mice. Triglyceride (TG), diacylglycerol (DAG), free fatty acid (FFA), phospholipids (PPL), and cholesterol esters (CE). (D) mRNA expression levels of *Fas*, *Srebp1c*, *Scd1*, *Scd4*, *Cd36*, *Lpl*, *Hsl*, *Pgc1a*, *Ppara*, *Pparg*, *Mcd1*, *Cpt1*, *Cpt2*, *Acadm*, *Dgat1*, *Dgat2* in the left ventricle of 12-14-week-old WT and *Bco2*^{-/-} female mice calculated using the $2^{-\Delta\Delta CT}$ method ($n = 4\text{--}6$ mice/genotype). (E) Immunoblot and quantification of cardiac CPT2 (125 kDa) in 12-14-week-old WT and *Bco2*^{-/-} female mice ($n = 3$ mice/genotype). Levels of vinculin (118 kDa) were used as the loading control. (F) Time until exhaustion (in seconds) during an inclined treadmill endurance test ($n = 3$ mice/genotype) in 12-week-old WT and *Bco2*^{-/-} female mice. Values are expressed as mean \pm SD. Statistical analysis by *t*-test between genotypes within each metabolite (A-C) or gene (D) or protein (E) or running time (F); * $p \leq .05$.

TABLE 2 Triglyceride acyl chains in the heart of WT and *Bco2^{-/-}* female mice

Acy chains	Wild-type	<i>Bco2^{-/-}</i>
14:0	16.1 ± 6.9	11.3 ± 2.8
16:0	387.4 ± 144.5	214.2 ± 40.0*
16:1	31.1 ± 11.6	20.1 ± 7.3
18:0	108.4 ± 40.0	62.4 ± 3.7*
18:1 n-9	513.2 ± 194.2	211.6 ± 51.5*
18:1 n-7	48.8 ± 15.0	20.6 ± 6.6*
18:2	541.9 ± 244.9	277.8 ± 69.9*
18:3 n-6	0.32 ± 0.13	0.28 ± 0.14
18:3 n-3	10.0 ± 4.3	4.6 ± 1.1*
20:0	6.2 ± 2.2	5.4 ± 0.30
20:1	16.7 ± 16.3	5.7 ± .81
20:4	25.1 ± 11.6	13.9 ± 2.3
20:5	0.21 ± 0.14	0.19 ± 0.7
22:6	4.02 ± 1.14	3.6 ± 1.0
22:0	3.1 ± 0.73	3.23 ± 0.40
24:0	0.05 ± 0.02	0.06 ± 0.03

Note: GC-MS analysis of triglyceride acyl chains (μg/g tissue) in the left ventricle of 14-week-old WT and *Bco2^{-/-}* female mice. Values are as means ± SD. *n* = 5/group. Statistical analysis by *t*-test between genotypes within each metabolite.

**p* ≤ .05.

(Figure 2E,F), and significantly increased the phosphorylation of PDH E1 alpha subunit at the S293 and S300 regulatory sites of the E1 alpha subunit (Figure 2G) and hence decreased the enzymatic activity of the PDH complex (Figure 2H). While the total kinase and phosphatase activities were not assessed, these data support the conclusion that retinoic acid regulates cardiac *Pdk4* expression and that these transcriptional changes translate into changes in the activity levels of its downstream target.

We also asked whether *Pdk4* was similarly regulated in other major metabolically active tissues, such as gastrocnemius muscle and liver, with high and low abundance of the PDK4 protein, respectively.⁴⁴ The gastrocnemius is a skeletal muscle with a mixed fiber type, even though with a predominant representation of the large fast twitch glycolytic Type IIB.⁷⁶ In WT mice, the expression of *Pdk4* remained unchanged in skeletal muscle when retinoic acid signaling was attenuated (Figure S1B) or the synthesis was enhanced (Figure S2B). Although we did not survey other skeletal muscles, it seems that the retinoid-dependent regulation of *Pdk4* in the heart is not shared by all types of muscle in the body. Prior studies indicated that hepatic *Pdk4* expression is attenuated upon dietary vitamin A deficiency in male and female rodents.^{77,78} Interestingly, Kang and colleagues⁷⁷ found that in mice fed a vitamin A deficient diet, retinoic acid treatment did not normalize *Pdk4* expression levels.

These authors concluded that the vitamin A deficient diet might decrease *Pdk4* expression in the murine liver through indirect mechanisms that do not involve retinoic acid levels or signaling per se. In our study, hepatic *Pdk4* was not affected by treatment with BMS493 (Figure S1A) but was upregulated by the administration of retinaldehyde (Figure S2A), suggesting a non-genomic effect of retinoids in the mouse liver.¹⁷ Notably, tissue-specific regulation of *Pdk4* has been reported.⁴⁴ Overall, our data strongly argue for the role of retinoic acid in the regulation of *Pdk4* specifically in the adult heart. The biological relevance of this regulation remains to be clarified. It is known that *Pdk4* and PDH activities fluctuate (decrease and increase, respectively) during the fast-refeeding transition.^{8,79-81} Interestingly, hepatic retinoic acid concentrations decline during refeeding.⁸² Thus, it is intriguing to speculate that if retinoic acid concentrations were to similarly fluctuate in the heart, a decline in cardiac levels of retinoic acid during the fasting-refeeding transition might well contribute to downregulate *Pdk4* and hence upregulate PDH activity.

The literature supports the notion that dietary carotenoids, including the vitamin A precursor β-carotene, are beneficial for heart health.^{24,25,83} BCO2 is the sole carotenoid cleavage enzyme expressed in the adult heart,³⁰ and deletion of *Bco2* in mice does not re-activate the expression of *Bco1* in the adult organ (data not shown). Retinoid and metabolic phenotypes, regardless of the availability of dietary carotenoids, have been extensively described in *Bco2^{-/-}* mice, particularly in liver, muscle, adipose, and hypothalamus.^{33,34,36,37,56,70,84} Our measurements of retinoid concentrations revealed a significant retinoic acid insufficiency in the mutant heart (but not in the liver nor serum; Figure 3A-C), with no changes in retinol and retinyl ester levels compared to WT controls (Table 1). Consistent with the low retinoic acid concentrations, cardiac levels of *Cyp26a1* mRNA were also reduced in the hearts of the mutant mice (Figure 3D). This gene encodes for one of the enzymes responsible for the catabolism of retinoic acid and is directly induced by retinoic acid.⁴⁸ We also found that *Raldh1* mRNA expression was increased in the heart of the *Bco2^{-/-}* mice (Figure 3D). RALDH1 is the pre-eminent postnatal retinaldehyde dehydrogenase that catalyzes the irreversible conversion of retinaldehyde to retinoic acid.^{54,85} We interpreted this upregulation as an attempt, albeit futile, to counteract the reduction in retinoic acid levels in the mutant heart. However, it cannot be unequivocally excluded that *Raldh1* may be regulated by additional factors that might change under oxidative stress, for example, as discussed further below. Alternatively, the *Raldh1* transcriptional changes in the mutant hearts may reflect other functions of the enzyme, which is known to oxidize lipid aldehydes, for instance.⁸⁶ LRAT is the main enzyme that synthesizes retinyl ester

stores in mammalian tissues^{87–89} and its transcription seems to be directly responsive to retinoic acid.⁹⁰ Since *Lrat* mRNA levels are often found to correlate with tissue retinoid status,⁹¹ we were surprised to detect increased levels of *Lrat* in the *Bco2*^{-/-} hearts despite the low tissue retinoic acid concentrations and the absence of differences in cardiac retinyl ester levels between WT and mutant mice (Table 1 and Figure 3A). However, a lack of correlation between LRAT mRNA and protein levels was reported in mouse liver.⁹² Currently, we cannot reconcile this discrepancy. Nevertheless, our data linked the cardiac retinoic acid insufficiency with reduced PDK4 mRNA and protein levels in the mutant heart (Figure 4). Indeed, restoring cardiac retinoid acid levels by N-Acetylcysteine (NAC) treatment (see more below) normalized the expression of *Pdk4* (Figure 5E–G).

Wondering why the lack of *Bco2* resulted in a selective cardiac retinoic acid insufficiency, we considered the mitochondria localization of the enzyme. On both carotenoid-supplemented and regular chow diets, *Bco2*^{-/-} mice displayed cellular oxidative stress as well as impaired mitochondrial functions, at least in the hypothalamus, liver, muscle, and adipose tissue.^{33,34,56,84} These findings suggest that BCO2 is not only protective against toxic carotenoid accumulation³² but could also play a carotenoid-independent role in the maintenance of mitochondrial redox balance and in keeping low oxidative stress and inflammatory levels,^{34,70} although the underlying mechanisms remain unclear. We confirmed alterations of the oxidative stress status and mitochondrial functioning in the heart of *Bco2*^{-/-} mice on the regular chow diet, without concomitant changes in mitochondrial content (Figure 5A) or respiratory chain complexes (Figure 5B). Interestingly, it has been reported that some of the key players of mitochondrial dynamics are regulated by retinoic acid, such as the dynamin-related protein DRP1.⁹³ In our findings, only *Mfn1* expression was slightly but significantly decreased in the heart of the *Bco2*^{-/-} mice (Figure 5C). In the heart, MFN1 is most effective at maintaining mitochondrial fusion, which suppresses ROS accumulation.⁵⁸ Hampered mitochondrial fusion can harm the cristae structure and inner mitochondrial membrane integrity, leading to the release of cytochrome c.^{94,95} Hence, measurement of MFN1 protein or mRNA expression is often used as a proxy for mitochondrial quality as well as ROS balance. It is not known whether retinoic acid regulates *Mfn1* expression. Nevertheless, the decrease in *Mfn1* in the heart of the *Bco2*^{-/-} mice suggests excessive ROS accumulation and/or production in the mutant heart. The enhanced cardiac expression of *Alcat1* and *p22phox* (Figure 5C), both of which are inducible in the presence of high levels of ROS,^{61,62} concurs with this interpretation. Therefore, we hypothesized that the retinoic acid insufficiency in

the heart of the mutant mice could have resulted from its spontaneous catabolism in the highly oxidative environment of the cardiac tissue. Notably, treatment with Mitotempo, a mitochondria-specific antioxidant agent derivative of MitoQ, was shown to be effective in alleviating mitochondrial oxidative stress in various tissues of the *Bco2*^{-/-} mice.³⁴ Our treatment of the mutant mice with NAC, a potent antioxidant and ROS scavenger⁶³ albeit not mitochondria-specific, confirmed that indeed this was the case. After two weeks of treatment, NAC restored retinoic acid levels as well as *Pdk4* mRNA and protein expression in the heart of the *Bco2*^{-/-} mice (Figure 5F,G) without affecting retinoic acid levels in the mutant liver (Figure S5), and without perturbing retinoic acid levels and *Pdk4* status in the heart of the WT control group (Figure 5E,F). In this mutant strain, the cardiac retinoic acid insufficiency is secondary to oxidative stress. Nevertheless, the *Bco2*^{-/-} mouse model supports a role for retinoic acid in regulating the PDK4/PDH pathway in the heart.

Whereas the lack of *Bco2* did not affect the expression of *Pdk4* in skeletal muscle (gastrocnemius; Figure S4C), a surprising finding was the reduction of *Pdk4* expression in the liver of the mutant mice (Figure S4B) without changes in hepatic retinoic acid concentration (Figure 3B). These data, as well as the above-mentioned inconsistent response of hepatic *Pdk4* in WT mice subjected to BMS or retinaldehyde treatments (Figures S1A and S2A), confirm the organ-specific transcriptional regulation of *Pdk4* by retinoic acid and imply that the expression of this gene in the liver might be dependent on multiple factors that remain to be identified.

Retinoic acid is not the only regulator of PDK4. Indeed, its expression can be modulated *in vivo* by many different factors including sex hormones, insulin signaling, growth hormone, as well as starvation.^{6–9} Estrogen induces *Pdk4* expression,⁹⁶ and our studies were conducted only in adult female mice that do have an estrous cycle. However, measurements of *Pdk4* expression in the *Bco2*^{-/-} and WT strain at pre-puberty, i.e., in absence of an estrous cycle or measurable estrogen levels,⁹⁷ also yielded similar results (Figure S4A). Moreover, preliminary analyses revealed attenuation of *Pdk4* expression in the heart of adult mutant males compared to WT controls on the regular chow diet (data not shown). Thus, we argue that the retinoid-dependent regulation of cardiac *Pdk4* is not dimorphic, nor influenced by sex hormones, likely not by estrogen.

The attenuation of *Pdk4* mRNA levels in the heart of the *Bco2*^{-/-} mice, translated into decreased phosphorylation and increased enzymatic activity of the PDH complex (Figure 4), implying increased acetyl-CoA synthesis from pyruvate.^{4,98} Overall, our data pointed toward an inherent cardiac reprogramming of fuel preference (glucose over fat) in the mutant heart driven by the retinoic

acid-mediated transcriptional changes (of *Pdk4*) occurring rather specifically in this organ. However, as the model employed here is a whole-body knockout, we cannot exclude indirect effects of the lack of *Bco2* in other organs (liver or intestine, for instance) that could influence the availability of circulating substrates. Serum triglyceride levels were significantly lower in the *Bco2*^{-/-} mice (Figure 7A), perhaps an indication of reduced delivery of exogenous fuel, i.e., lipids, to the heart which indeed also showed reduced TG concentration, including 18:2 and 18:3 fatty acids, exclusively dietarily derived (Figure 7C and Table 2). Hepatic lipid metabolism was shown to be impaired in mice lacking *Bco2*,^{31,33,56} but these reports are inconsistent. For instance, in one report *Bco2*^{-/-} mice displayed a trend toward an increase in hepatic triglyceride levels accompanied by enhanced gene expression and protein levels of SREBP1c, ACC, and APOB, interpreted as an increase in fatty acid oxidation.³⁴ Another report instead showed a decrease in hepatic lipid species.⁵⁶ However, it is not known whether the lack of *Bco2* impairs lipid secretion from the liver and/or intestine. Lipid metabolism was also found to be altered in the adipose depot of the mutant strain, but this was studied only following supplementation with carotenoids.³⁵ Higher blood glucose levels and evidence of insulin resistance have been typically reported in *Bco2*^{-/-} mice.^{34,56,70} Here, we found that serum glucose levels in the mutants were unaffected in the fasting state and slightly decreases in fed mice (Figure 6A). Based on these data, it is hard to know whether glucose availability and/or utilization may be altered in the *Bco2*^{-/-} mice. However, the increase in serum lactate levels (Figure 6B) seems consistent with the expected increased glycolysis in these mice. Notably, tissue lipid and glucose metabolism have been mostly characterized in *Bco2*^{-/-} male mice,^{34,56,70} whereas ours is the only study conducted in mutant adult females.

Our data also provide evidence, although indirect, of disrupted lipid metabolism in the heart of the *Bco2*^{-/-} mice, such as reduced FA synthesis (attenuated *Srebp1c* and *Scd4*, reduced levels of 16:0, 18:0, and 18:1 fatty acid species; Figure 7D and Table 2), as well as potentially impaired fatty acid oxidation (attenuation of *Acdam* and *Cpt2*; Figure 7D). The current data cannot unequivocally establish whether these altered lipid pathways in the heart of the mutants are a direct consequence of the lack of *Bco2* or if they are mechanisms developed to compensate for enhanced PDH activity (for instance, reduced FA synthesis could spare acetyl-CoA as a substrate for the TCA cycle). Furthermore, these alterations could also be more directly the result of the retinoic acid insufficiency in this organ, but it is not known whether the above-mentioned genes may be regulated by retinoic acid in the heart. Similar reasoning could also apply to the increase

in *Glut1* and *Mct1*, both essential to the translocation and metabolism of glucose and lactate, respectively^{99,100} (Figure 6C). Importantly, though, these cardiac metabolic alterations of the *Bco2*^{-/-} mice are physiologically relevant as the mutants, which are viable and fertile under normal housing conditions, showed a marked decrease in exercise capacity (Figure 7F). Since *Pdk4* expression was not attenuated in the skeletal muscle of the *Bco2*^{-/-} mice (Figure S4C), we inferred that this phenotype is mainly dependent on the metabolic deficit of the mutant heart reflecting its inability to adapt to different energy-providing substrates (lipid versus glucose) depending on energy demand (as in the case of exercise). The elevated cardiac oxidative stress also likely contributes to the reduced exercise endurance of the mutant mice.

In summary, these data revealed novel critical insights into the regulation of cardiac metabolic flexibility by retinoic acid, and more generally into the effects of retinoid and carotenoid metabolism on heart health. Our findings warrant further investigations into the role of retinoic acid as a regulator of adult organ functions.

AUTHOR CONTRIBUTIONS

Chelsee Holloway: investigation, data curation, and interpretation, writing—original draft preparation, reviewing, and editing; Guo Zhong: method, data curation, and interpretation; Youn-Kyung Kim: investigation, writing—reviewing and editing; Hong Ye: investigation; Harini Sampath: method, data curation, interpretation, writing—reviewing and editing; Ulrich Hammerling: data interpretation, writing—reviewing and editing; Nina Isoherranen: method, data curation, interpretation, writing—reviewing and editing; Loredana Quadro: conceptualization, data curation, interpretation, writing—original and final draft preparation, reviewing and editing.

ACKNOWLEDGMENTS

We thank Dr. Robert A. Harris for his guidance in identifying a suitable anti-PDK4 antibody. This work was supported by the U.S National Institute of Health (NIH) F31 Ruth Kirschstein Predoctoral Individual Research Service Award 1F31HL143930 (to CH), by the 2020 and 2021 Rutgers Center for Lipid Research (RCLR) small grant (to CH) and partially by the NIH R01 HD094778 (to LQ), GM111772 (to NI) and DK126963 (to HS). This work was also partially supported by the USDA National Institute of Food and Agriculture, Hatch project, accession number 1018402 (to LQ). The content of this manuscript is solely the responsibility of the authors and does not necessarily represent the official views of the NIH.

DISCLOSURES

The authors declare no conflict of interest for this work.

DATA AVAILABILITY STATEMENT

All the data that support the findings of this study are available in the manuscript, including methods and/or supplementary material.

ORCID

Loredana Quadro  <https://orcid.org/0000-0002-2811-9594>

REFERENCES

- Schulze PC, Drosatos K, Goldberg IJ. Lipid use and misuse by the heart. *Circ Res*. 2016;118:1736-1751.
- Chambers KT, Leone TC, Sambandam N, et al. Chronic inhibition of pyruvate dehydrogenase in heart triggers an adaptive metabolic response. *J Biol Chem*. 2011;286:11155-11162.
- Liu LX, Rowe GC, Yang S, et al. PDK4 inhibits cardiac pyruvate oxidation in late pregnancy. *Circ Res*. 2017;121:1370-1378.
- Patel MS, Korotchkina LG. Regulation of the pyruvate dehydrogenase complex. *Biochem Soc Trans*. 2006;34:217-222.
- Harris RA, Bowker-Kinley MM, Huang B, Wu P. Regulation of the activity of the pyruvate dehydrogenase complex. *Adv Enzyme Regul*. 2002;42:249-259.
- Wende AR, Huss JM, Schaeffer PJ, Giguere V, Kelly DP. PGC-1alpha coactivates PDK4 gene expression via the orphan nuclear receptor ERRalpha: a mechanism for transcriptional control of muscle glucose metabolism. *Mol Cell Biol*. 2005;25:10684-10694.
- Connaughton S, Chowdhury F, Attia RR, et al. Regulation of pyruvate dehydrogenase kinase isoform 4 (PDK4) gene expression by glucocorticoids and insulin. *Mol Cell Endocrinol*. 2010;315:159-167.
- Wu P, Sato J, Zhao Y, Jaskiewicz J, Popov KM, Harris RA. Starvation and diabetes increase the amount of pyruvate dehydrogenase kinase isoenzyme 4 in rat heart. *Biochem J*. 1998;329(Pt 1):197-201.
- Attia RR, Connaughton S, Boone LR, et al. Regulation of pyruvate dehydrogenase kinase 4 (PDK4) by thyroid hormone: role of the peroxisome proliferator-activated receptor gamma coactivator (PGC-1 alpha). *J Biol Chem*. 2010;285:2375-2385.
- Jensen SK, Yates B, Lyden E, Krogstrand KS, Hanson C. Dietary micronutrient intake of participants in a “partners together in health” cardiac rehabilitation intervention. *J Cardiopulm Rehabil Prev*. 2018;38:388-393.
- Kkeveetil CV, Thomas G, Chander SJU. Role of micronutrients in congestive heart failure: a systematic review of randomized controlled trials. *Ci Ji Yi Xue Za Zhi*. 2016;28:143-150.
- Wong AP, Niedzwiecki A, Rath M. Myocardial energetics and the role of micronutrients in heart failure: a critical review. *Am J Cardiovasc Dis*. 2016;6:81-92.
- Brazionis L, Walker KZ, Itsopoulos C, O'Dea K. Plasma retinol: a novel marker for cardiovascular disease mortality in Australian adults. *Nutr Metab Cardiovasc Dis*. 2012;22:914-920.
- Gey KF, Ducimetiere P, Evans A, et al. Low plasma retinol predicts coronary events in healthy middle-aged men: the PRIME Study. *Atherosclerosis*. 2010;208:270-274.
- Huang J, Weinstein SJ, Yu K, Mannisto S, Albanez D. Association between serum retinol and overall and cause-specific mortality in a 30-year prospective cohort study. *Nat Commun*. 2021;12:6418.
- Yu Y, Zhang H, Song Y, et al. Plasma retinol and the risk of first stroke in hypertensive adults: a nested case-control study. *Am J Clin Nutr*. 2019;109:449-456.
- Iskakova M, Karbyshev M, Piskunov A, Rochette-Egly C. Nuclear and extranuclear effects of vitamin A. *Can J Physiol Pharmacol*. 2015;93:1065-1075.
- Sirbu IO, Chis AR, Moise AR. Role of carotenoids and retinoids during heart development. *Biochim Biophys Acta Mol Cell Biol Lipids*. 2020;1865:158636.
- Choudhary R, Palm-Leis A, Scott RC 3rd, et al. All-trans retinoic acid prevents development of cardiac remodeling in aortic banded rats by inhibiting the renin-angiotensin system. *Am J Physiol Heart Circ Physiol*. 2008;294:H633-H644.
- Manolescu DC, Jankowski M, Danalache BA, et al. All-trans retinoic acid stimulates gene expression of the cardioprotective natriuretic peptide system and prevents fibrosis and apoptosis in cardiomyocytes of obese ob/ob mice. *Appl Physiol Nutr Metab*. 2014;39:1127-1136.
- Paiva SA, Matsubara LS, Matsubara BB, et al. Retinoic acid supplementation attenuates ventricular remodeling after myocardial infarction in rats. *J Nutr*. 2005;135:2326-2328.
- Distel E, Cadoudal T, Collinet M, Park EA, Benelli C, Bortoli S. Early induction of pyruvate dehydrogenase kinase 4 by retinoic acids in adipocytes. *Mol Nutr Food Res*. 2017;61. <https://doi.org/10.1002/mnfr.201600920>
- Kwon HS, Huang B, Ho Jeoung N, Wu P, Steussy CN, Harris RA. Retinoic acids and trichostatin A (TSA), a histone deacetylase inhibitor, induce human pyruvate dehydrogenase kinase 4 (PDK4) gene expression. *Biochim Biophys Acta*. 2006;1759:141-151.
- Karppi J, Laukkonen JA, Makikallio TH, Ronkainen K, Kurl S. Low beta-carotene concentrations increase the risk of cardiovascular disease mortality among Finnish men with risk factors. *Nutr Metab Cardiovasc Dis*. 2012;22:921-928.
- Cheng HM, Koutsidis G, Lodge JK, Ashor AW, Siervo M, Lara J. Lycopene and tomato and risk of cardiovascular diseases: a systematic review and meta-analysis of epidemiological evidence. *Crit Rev Food Sci Nutr*. 2019;59:141-158.
- Karppi J, Kurl S, Makikallio TH, Ronkainen K, Laukkonen JA. Serum beta-carotene concentrations and the risk of congestive heart failure in men: a population-based study. *Int J Cardiol*. 2013;168:1841-1846.
- Quadro L, Giordano E, Costabile BK, et al. Interplay between beta-carotene and lipoprotein metabolism at the maternal-fetal barrier. *Biochim Biophys Acta Mol Cell Biol Lipids*. 2020;1865:158591.
- Blaner WS, Li Y, Brun PJ, Yuen JJ, Lee SA, Clugston RD. Vitamin A absorption, storage and mobilization. *Subcell Biochem*. 2016;81:95-125.
- Harrison EH, Quadro L. Apocarotenoids: emerging roles in mammals. *Annu Rev Nutr*. 2018;38:153-172.
- Lindqvist A, He YG, Andersson S. Cell type-specific expression of beta-carotene 9',10'-monooxygenase in human tissues. *J Histochem Cytochem*. 2005;53:1403-1412.
- Amengual J, Lobo GP, Golczak M, et al. A mitochondrial enzyme degrades carotenoids and protects against oxidative stress. *FASEB J*. 2011;25:948-959.

32. Lobo GP, Isken A, Hoff S, Babino D, von Lintig J. BCDO2 acts as a carotenoid scavenger and gatekeeper for the mitochondrial apoptotic pathway. *Development*. 2012;139:2966-2977.
33. Wu L, Guo X, Hartson SD, et al. Lack of beta, beta-carotene-9', 10'-oxygenase 2 leads to hepatic mitochondrial dysfunction and cellular oxidative stress in mice. *Mol Nutr Food Res*. 2017;61:1600576.
34. Wu L, Lu P, Guo X, et al. β -carotene oxygenase 2 deficiency-triggered mitochondrial oxidative stress promotes low-grade inflammation and metabolic dysfunction. *Free Radic Biol Med*. 2021;164:271-284.
35. Ip BC, Liu C, Lichtenstein AH, von Lintig J, Wang XD. Lycopene and apo-10'-lycopenoic acid have differential mechanisms of protection against hepatic steatosis in beta-carotene-9', 10'-oxygenase knockout male mice. *J Nutr*. 2015;145:268-276.
36. Spiegler E, Kim YK, Hoyos B, et al. beta-apo-10'-carotenoids support normal embryonic development during vitamin A deficiency. *Sci Rep*. 2018;8:8834.
37. Amengual J, Widjaja-Adhi MAK, Rodriguez-Santiago S, et al. Two carotenoid oxygenases contribute to mammalian provitamin A metabolism. *J Biol Chem*. 2013;288:34081-34096.
38. Kim YK, Quadro L. Reverse-phase high-performance liquid chromatography (HPLC) analysis of retinol and retinyl esters in mouse serum and tissues. *Methods Mol Biol*. 2010;652:263-275.
39. Zhong G, Hogarth C, Snyder JM, et al. The retinoic acid hydroxylase Cyp26a1 has minor effects on postnatal vitamin A homeostasis, but is required for exogenous atRA clearance. *J Biol Chem*. 2019;294:11166-11179.
40. Honarbakhsh M, Ericsson A, Zhong G, et al. Impact of vitamin A transport and storage on intestinal retinoid homeostasis and functions. *J Lipid Res*. 2021;62:100046.
41. Komakula SSB, Tumova J, Kumaraswamy D, et al. The DNA repair protein OGG1 protects against obesity by altering mitochondrial energetics in white adipose tissue. *Sci Rep*. 2018;8:14886.
42. Bradford MM. A rapid and sensitive method for the quantitation of microgram quantities of protein utilizing the principle of protein-dye binding. *Anal Biochem*. 1976;72:248-254.
43. Linn TC, Pelley JW, Pettit FH, Hucho F, Randall DD, Reed LJ. -Keto acid dehydrogenase complexes. XV. Purification and properties of the component enzymes of the pyruvate dehydrogenase complexes from bovine kidney and heart. *Arch Biochem Biophys*. 1972;148:327-342.
44. Klyuyeva A, Tuganova A, Kedishvili N, Popov KM. Tissue-specific kinase expression and activity regulate flux through the pyruvate dehydrogenase complex. *J Biol Chem*. 2019;294:838-851.
45. Folch J, Lees M, Sloane Stanley GH. A simple method for the isolation and purification of total lipides from animal tissues. *J Biol Chem*. 1957;226:497-509.
46. Sharma P, Wu G, Kumaraswamy D, et al. Sex-dependent effects of 7,8-dihydroxyflavone on metabolic health are associated with alterations in the host gut microbiome. *Nutrients*. 2021;13:637.
47. Burchat N, Akal T, Ntambi JM, Trivedi N, Suresh R, Sampath H. SCD1 is nutritionally and spatially regulated in the intestine and influences systemic postprandial lipid homeostasis and gut-liver crosstalk. *Biochim Biophys Acta Mol Cell Biol Lipids*. 2022;1867:159195.
48. Isoherranen N, Zhong G. Biochemical and physiological importance of the CYP26 retinoic acid hydroxylases. *Pharmacol Ther*. 2019;204:107400.
49. Chen F, Shao F, Hinds A, et al. Retinoic acid signaling is essential for airway smooth muscle homeostasis. *JCI Insight*. 2018;3:e120398.
50. de The H, Vivanco-Ruiz MM, Tiollais P, Stunnenberg H, Dejean A. Identification of a retinoic acid responsive element in the retinoic acid receptor beta gene. *Nature*. 1990;343:177-180.
51. Sucov HM, Murakami KK, Evans RM. Characterization of an autoregulated response element in the mouse retinoic acid receptor type beta gene. *Proc Natl Acad Sci U S A*. 1990;87:5392-5396.
52. Huang B, Wu P, Popov KM, Harris RA. Starvation and diabetes reduce the amount of pyruvate dehydrogenase phosphatase in rat heart and kidney. *Diabetes*. 2003;52:1371-1376.
53. Belyaeva OV, Adams MK, Popov KM, Kedishvili NY. Generation of retinaldehyde for retinoic acid biosynthesis. *Biomolecules*. 2019;10:5.
54. Napoli JL. Post-natal all-trans-retinoic acid biosynthesis. *Methods Enzymol*. 2020;637:27-54.
55. Wassef L, Shete V, Costabile B, Rodas R, Quadro L. High preformed vitamin A intake during pregnancy prevents embryonic accumulation of intact beta-carotene from the maternal circulation in mice. *J Nutr*. 2015;145:1408-1414.
56. Wu L, Guo X, Lyu Y, et al. Targeted metabolomics reveals abnormal hepatic energy metabolism by depletion of beta-carotene oxygenase 2 in mice. *Sci Rep*. 2017;7:14624.
57. Chan DC. Fusion and fission: interlinked processes critical for mitochondrial health. *Annu Rev Genet*. 2012;46:265-287.
58. Lee JY, Kapur M, Li M, et al. MFN1 deacetylation activates adaptive mitochondrial fusion and protects metabolically challenged mitochondria. *J Cell Sci*. 2014;127:4954-4963.
59. Chen H, Vermulst M, Wang YE, et al. Mitochondrial fusion is required for mtDNA stability in skeletal muscle and tolerance of mtDNA mutations. *Cell*. 2010;141:280-289.
60. Han Y, Kim B, Cho U, et al. Mitochondrial fission causes cisplatin resistance under hypoxic conditions via ROS in ovarian cancer cells. *Oncogene*. 2019;38:7089-7105.
61. Liu X, Ye B, Miller S, et al. Ablation of ALCAT1 mitigates hypertrophic cardiomyopathy through effects on oxidative stress and mitophagy. *Mol Cell Biol*. 2012;32:4493-4504.
62. Becker JS, Adler A, Schneeberger A, et al. Hyperhomocysteinemia, a cardiac metabolic disease: role of nitric oxide and the p22phox subunit of NADPH oxidase. *Circulation*. 2005;111:2112-2118.
63. Zhitkovich A. N-acetylcysteine: antioxidant, aldehyde scavenger, and more. *Chem Res Toxicol*. 2019;32:1318-1319.
64. Chandel NS. Glycolysis. *Cold Spring Harb Perspect Biol*. 2021;13:a040535.
65. Goldstein JL, DeBose-Boyd RA, Brown MS. Protein sensors for membrane sterols. *Cell*. 2006;124:35-46.
66. Miyazaki M, Jacobson MJ, Man WC, et al. Identification and characterization of murine SCD4, a novel heart-specific stearoyl-CoA desaturase isoform regulated by leptin and dietary factors. *J Biol Chem*. 2003;278:33904-33911.
67. Di W, Lv J, Jiang S, et al. PGC-1: the energetic regulator in cardiac metabolism. *Curr Issues Mol Biol*. 2018;28:29-46.
68. Houten SM, Wanders RJ. A general introduction to the biochemistry of mitochondrial fatty acid beta-oxidation. *J Inherit Metab Dis*. 2010;33:469-477.

69. Yang N, Parker LE, Yu J, et al. Cardiac retinoic acid levels decline in heart failure. *JCI Insight*. 2021;6:e137593.
70. Guo X, Wu L, Lyu Y, et al. Ablation of beta,beta-carotene-9',10'-oxygenase 2 remodels the hypothalamic metabolome leading to metabolic disorders in mice. *J Nutr Biochem*. 2017;46:74-82.
71. Smith RL, Soeters MR, Wust RCI, Houtkooper RH. Metabolic flexibility as an adaptation to energy resources and requirements in health and disease. *Endocr Rev*. 2018;39:489-517.
72. Lopaschuk GD, Karwi QG, Tian R, Wende AR, Abel ED. Cardiac energy metabolism in heart failure. *Circ Res*. 2021;128:1487-1513.
73. Zhao G, Jeoung NH, Burgess SC, et al. Overexpression of pyruvate dehydrogenase kinase 4 in heart perturbs metabolism and exacerbates calcineurin-induced cardiomyopathy. *Am J Physiol Heart Circ Physiol*. 2008;294:H936-H943.
74. Mori J, Alrob OA, Wagg CS, Harris RA, Lopaschuk GD, Oudit GY. ANG II causes insulin resistance and induces cardiac metabolic switch and inefficiency: a critical role of PDK4. *Am J Physiol Heart Circ Physiol*. 2013;304:H1103-H1113.
75. Branco AF, Pereira SP, Gonzalez S, Gusev O, Rizvanov AA, Oliveira PJ. Gene expression profiling of H9c2 myoblast differentiation towards a cardiac-like phenotype. *PLoS One*. 2015;10:e0129303.
76. Peters SJ, Harris RA, Heigenhauser GJ, Spratt LL. Muscle fiber type comparison of PDH kinase activity and isoform expression in fed and fasted rats. *Am J Physiol Regul Integr Comp Physiol*. 2001;280:R661-R668.
77. Kang HW, Bhimidi GR, Odom DP, Brun PJ, Fernandez ML, McGrane MM. Altered lipid catabolism in the vitamin A deficient liver. *Mol Cell Endocrinol*. 2007;271:18-27.
78. McClintick JN, Crabb DW, Tian H, et al. Global effects of vitamin A deficiency on gene expression in rat liver: evidence for hypoandrogenism. *J Nutr Biochem*. 2006;17:345-355.
79. Jeoung NH, Wu P, Joshi MA, et al. Role of pyruvate dehydrogenase kinase isoenzyme 4 (PDHK4) in glucose homeostasis during starvation. *Biochem J*. 2006;397:417-425.
80. Holness MJ, Sugden MC. Pyruvate dehydrogenase activities during the fed-to-starved transition and on re-feeding after acute or prolonged starvation. *Biochem J*. 1989;258:529-533.
81. Sugden MC, Bulmer K, Gibbons GF, Holness MJ. Role of peroxisome proliferator-activated receptor-alpha in the mechanism underlying changes in renal pyruvate dehydrogenase kinase isoform 4 protein expression in starvation and after re-feeding. *Arch Biochem Biophys*. 2001;395:246-252.
82. Napoli JL. Retinoic acid: sexually dimorphic, anti-insulin and concentration-dependent effects on energy. *Nutrients*. 2022;14:1553.
83. Karppi J, Laukkanen JA, Makikallio TH, Ronkainen K, Kurl S. Serum beta-carotene and the risk of sudden cardiac death in men: a population-based follow-up study. *Atherosclerosis*. 2013;226:172-177.
84. Wu L, Guo X, Wang W, et al. Molecular aspects of beta, beta-carotene-9', 10'-oxygenase 2 in carotenoid metabolism and diseases. *Exp Biol Med (Maywood)*. 2016;241:1879-1887.
85. Kumar S, Sandell LL, Trainor PA, Koentgen F, Duester G. Alcohol and aldehyde dehydrogenases: retinoid metabolic effects in mouse knockout models. *Biochim Biophys Acta*. 2012;1821:198-205.
86. Kedishvili NY. Enzymology of retinoic acid biosynthesis and degradation. *J Lipid Res*. 2013;54:1744-1760.
87. O'Byrne SM, Wongsiriroj N, Libien J, et al. Retinoid absorption and storage is impaired in mice lacking lecithin:retinol acyltransferase (LRAT). *J Biol Chem*. 2005;280:35647-35657.
88. Batten ML, Imanishi Y, Maeda T, et al. Lecithin-retinol acyltransferase is essential for accumulation of all-trans-retinyl esters in the eye and in the liver. *J Biol Chem*. 2004;279:10422-10432.
89. Liu L, Gudas LJ. Disruption of the lecithin:retinol acyltransferase gene makes mice more susceptible to vitamin A deficiency. *J Biol Chem*. 2005;280:40226-40234.
90. Zolfaghari R, Ross AC. An essential set of basic DNA response elements is required for receptor-dependent transcription of the lecithin:retinol acyltransferase (Lrat) gene. *Arch Biochem Biophys*. 2009;489:1-9.
91. Ross AC, Zolfaghari R. Regulation of hepatic retinol metabolism: perspectives from studies on vitamin A status. *J Nutr*. 2004;134:269S-275S.
92. Saeed A, Yang J, Heegsma J, et al. Farnesoid X receptor and bile acids regulate vitamin A storage. *Sci Rep*. 2019;9:19493.
93. Chidipi B, Shah SI, Reiser M, et al. All-trans retinoic acid increases DRP1 levels and promotes mitochondrial fission. *Cell*. 2021;10:1202.
94. Chen Y, Liu Y, Dorn GW 2nd. Mitochondrial fusion is essential for organelle function and cardiac homeostasis. *Circ Res*. 2011;109:1327-1331.
95. Hsiao YT, Shimizu I, Wakasugi T, et al. Cardiac mitofusin-1 is reduced in non-responding patients with idiopathic dilated cardiomyopathy. *Sci Rep*. 2021;11:6722.
96. Zhang Y, Ma K, Sadana P, et al. Estrogen-related receptors stimulate pyruvate dehydrogenase kinase isoform 4 gene expression. *J Biol Chem*. 2006;281:39897-39906.
97. Safranski TJ, Lamberson WR, Keisler DH. Correlations among three measures of puberty in mice and relationships with estradiol concentration and ovulation. *Biol Reprod*. 1993;48:669-673.
98. Fernie AR, Carrari F, Sweetlove LJ. Respiratory metabolism: glycolysis, the TCA cycle and mitochondrial electron transport. *Curr Opin Plant Biol*. 2004;7:254-261.
99. Aerni-Flessner L, Abi-Jaoude M, Koenig A, Payne M, Hruz PW. GLUT4, GLUT1, and GLUT8 are the dominant GLUT transcripts expressed in the murine left ventricle. *Cardiovasc Diabetol*. 2012;11:63.
100. Bonen A. The expression of lactate transporters (MCT1 and MCT4) in heart and muscle. *Eur J Appl Physiol*. 2001;86:6-11.

SUPPORTING INFORMATION

Additional supporting information can be found online in the Supporting Information section at the end of this article.

How to cite this article: Holloway C, Zhong G, Kim Y-K, et al. Retinoic acid regulates pyruvate dehydrogenase kinase 4 (*Pdk4*) to modulate fuel utilization in the adult heart: Insights from wild-type and β -carotene 9',10' oxygenase knockout mice. *The FASEB Journal*. 2022;36:e22513.

doi: [10.1096/fj.202101910RR](https://doi.org/10.1096/fj.202101910RR)